

# Promotion Effects in Co-based Fischer–Tropsch Catalysis

---

BY FERNANDO MORALES AND BERT M. WECKHUYSEN

*Department of Inorganic Chemistry and Catalysis, Utrecht University, Debye Institute, Sorbonnelaan 16, Utrecht 3584 CA, The Netherlands*

## 1 General Introduction

**1.1 Fischer–Tropsch Synthesis.** – Franz Fischer, head of the Max-Planck Institut für Kohlenforschung in Mülheim (Germany) and Hans Tropsch, a co-worker of Fischer and professor of chemistry in Prague (Czech Republic), Mülheim (Germany) and Chicago (Illinois, USA), discovered in 1922 a catalytic reaction between CO and H<sub>2</sub>, which yields mixtures of higher alkanes and alkenes.<sup>1–20</sup> This invention made it possible for Germany to produce fuels from its coal reserves and by 1938 9 Fischer–Tropsch (F–T) plants were in operation making use of, *e.g.*, cobalt-based F–T catalysts. The expansion of these plants stopped around 1940, but existing plants continued to operate during World War II. It is worthwhile to notice that in 1944, Japan was operating 3 F–T plants based on coal reserves. Whilst being a major scientific as well as a technical success, the F–T process could not compete economically with the refining process of crude oil, becoming important starting from the 1950s. All this coincided with major discoveries of oil fields in the Middle East and consequently the price of crude oil dropped. Although a new F–T plant was built in Brownsville (Texas, USA) in 1950, the sharp increase in the price of methane caused the plant to shut down. Thus, due to bad economics F–T technology became of little importance for the industrial world after World War II and no new F–T plants were constructed. An exception was South-Africa, which started making fuels and chemicals from gasified coal based on the F–T process a half century ago due to embargoes initiated by the country's apartheid policies. Till today, South Africa's Sasol (South African Coal, Oil and Gas Corporation, Ltd.), building its first commercial F–T plant in 1955, is known as a major player in this field.<sup>21</sup>

It is remarkable to notice that there is today a renewed interest in F–T technology mainly due to:

- (i) The rising costs of crude oil. For some time now, the oil prices are well above \$50 per barrel.

- (ii) The drive to supply environmentally friendly automotive fuels, more in particular, the production of synthetic sulphur-free diesel, especially interesting for the European car fleet.
- (iii) The commercialisation of otherwise unmarketable natural gas at remote locations. CO<sub>2</sub> emission regulations will certainly lead in the future to a ban on natural gas flaring near crude oil production wells.

This all has led to the recent decisions on major investments by big petrochemical companies, such as Shell<sup>22</sup> and ExxonMobil,<sup>23</sup> to build large scale F–T plants in Qatar. This will result in an important shift from crude oil to natural gas as feedstock for the production of fuels and chemicals in the decades to come.<sup>24–27</sup> Industry projections estimate that by 2020 5% of the production of chemicals could be based on F–T technology with methane instead of crude oil refining operations. All this is especially promising in view of the long-term reserves of coal, which are estimated to be more than 20 times that of crude oil and coal is still used as the carbon source at the largest and economically successful F–T complex, namely the plants Sasol One to Three near Sasolburg in South Africa.<sup>21</sup> A picture of a Sasol Fischer–Tropsch plant is shown in Figure 1.<sup>28</sup>

The stoichiometry of the F–T process can be derived from the following two reactions, the polymerization reaction to produce hydrocarbon chains (1), and the water-gas shift reaction (2):



**Figure 1** Picture of a Sasol Fischer–Tropsch plant in South-Africa

The overall stoichiometry in case reaction (2) is completely driven to the right is:



With  $\Delta H_{227} = -204.8$  kJ, while the maximum attainable yield is 208.5 g of alkenes  $\text{C}_n\text{H}_{2n}$  per  $\text{Nm}^3$  of a mixture of 2 CO and  $\text{H}_2$  for complete conversion.<sup>29,30</sup> The CO/ $\text{H}_2$  is usually called synthesis gas, or in short syngas. The production of syngas, either by partial oxidation or steam reforming, can account for over 60% of the total cost of the F–T complex since the gasification process is highly endothermic and therefore a high-energy input is required.<sup>29–31</sup> It should also be clear that the carbon source used, being it either coal or natural gas, is available at low cost, while the gasification of methane is much more efficient than that of coal since coal simply has a much lower hydrogen content. The syngas produced is then fed into a F–T reactor, which converts it into a paraffin wax that is subsequently hydrocracked to make a variety of chemicals, at present mostly diesel, but also some naphtha, lubricants and gases. A scheme of the F–T reaction process, including syngas production and hydrocracking of the wax, is given in Figure 2.

The F–T reaction involves the following main steps at the catalyst surface:

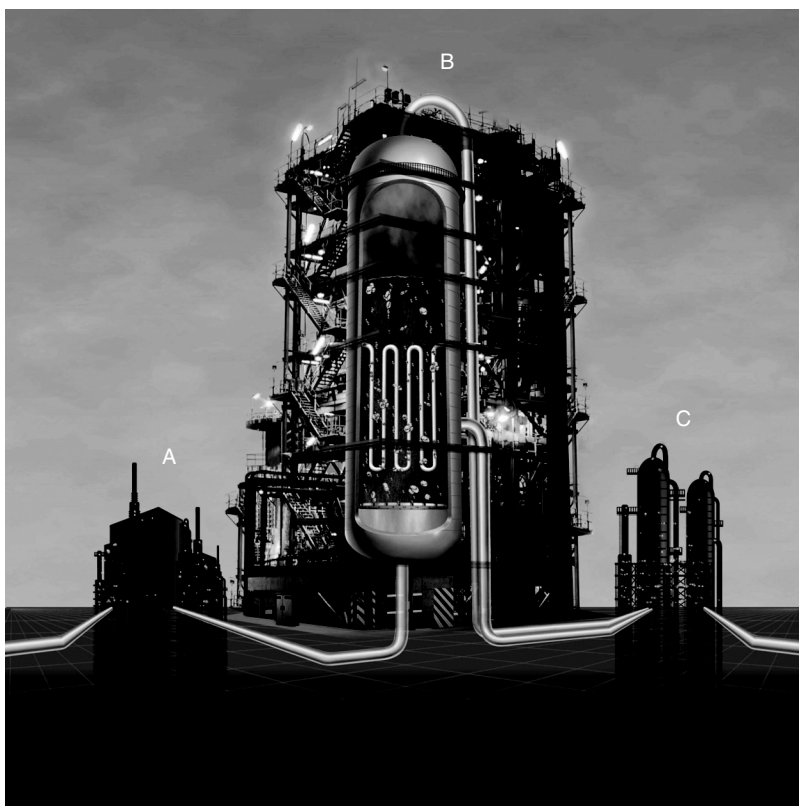
- (i) The adsorption and maybe dissociation of CO;
- (ii) The adsorption and dissociation of  $\text{H}_2$ ;
- (iii) Surface reactions leading to alkyl chains, which may terminate by the addition or elimination of hydrogen, giving rise to either paraffin or olefin formation.
- (iv) Desorption of the final hydrocarbon products, which can be considered as the primary products of the F–T process.
- (v) Secondary reactions taking place on the primary hydrocarbon products formed due to, *e.g.*, olefin readsorption followed by hydrogenation or chain growth reinitiation.

Various detailed mechanisms have been proposed and this matter still remains a controversial issue in the literature.

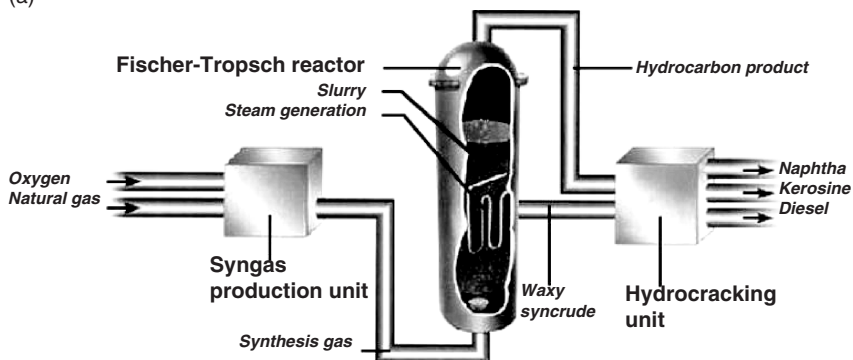
Some of the scientific questions that arise are:

- (i) Does the adsorbed CO molecule first dissociate into chemisorbed carbon and oxygen atoms? The chemisorbed carbon formed can then be hydrogenated to surface methyl and methylene groups in subsequent steps. Chain growth occurs by stepwise addition of  $\text{C}_1$  monomers to a surface alkyl group.
- (ii) Is the adsorbed CO molecule hydrogenated to a CHO or HCOH species, which inserts in the growing hydrocarbon chain?
- (iii) Is CO directly inserted in the growing chain and then subsequently hydrogenated?

It should be clear that a discussion on the F–T mechanism is beyond the scope of this paper and we refer the interested reader to several review papers on this topic.<sup>32–42,6,14</sup> In this respect, it is noteworthy to mention the excellent



(a)



(b)

**Figure 2** (a) Picture illustrating the different steps in the Fischer–Tropsch process: syngas production (A), hydrocarbon formation (B) and hydrocarbon production and (C) product upgrade and (b) detailed flow chart of the Fischer–Tropsch process

updates by Dry on the challenges and technological implementations of Co F–T synthesis.<sup>17–20</sup>

The overall selectivity of the F–T process is intimately related to the production of methane, which is not economic, since the back conversion to

syngas encounters, severe thermal and yield penalties. Consequently, substantial research efforts have been devoted to decrease the methane production by adjusting the catalyst composition. It is generally considered that the choice of the catalyst material is central to the F–T process. The latest generation of F–T catalysts are based on cobalt and the cobalt nanoparticles are usually supported on an oxide support, mostly silica, alumina and titania, while some promoters are added to the catalyst material in order to enhance the Co dispersion, *e.g.*, some noble metals. Other metal oxide promoters are often added to the catalysts to improve the F–T selectivity, *e.g.*, decreasing the methane production. Reducing the amount of promoter, especially in the case of noble metals, as well as the amount of cobalt are ways to reduce the catalyst production costs and it may be of no wonder that large research efforts in both academia and industrial laboratories have focused on finding the best performing, durable, but still cheap F–T catalyst formulation. Almost every industrial player in the F–T field has its own catalyst formulation, and is – as expected – very secretive about their exact composition of matter in the catalyst materials applied in pilot and/or industrial plants. The choice of the catalyst material is also related to the type of reactor used. In this respect, it is relevant to mention that Shell and BP use fixed bed reactors, whereas Sasol/Chevron and Exxon Mobil make use of slurry phase reactors. The latter plants require the continuous addition of catalyst material.

**1.2 Scope of the Review Paper.** – From the above reasoning it is clear that over the past decades a large number of studies have been reported on supported cobalt F–T catalysts. All these studies indicate that the number of available surface cobalt metal atoms determines the catalyst activity and attempts to enhance the catalytic activity have been focusing on two interconnected issues: (1) to reduce the cobalt-support oxide interaction and (2) to enhance the number of accessible cobalt atoms available for F–T reaction. It has been shown that the number of catalytically active cobalt atoms as well as their selectivity can be largely enhanced by the addition of small amounts of various elements, called promoters, to the catalyst material. The exact role of these promoters – as is the case for many other heterogeneous catalysts as well – remains often, however, unclear.

The aim of this review paper is to give an extensive overview of the different promoters used to develop new or improved Co-based F–T catalysts. Special attention is directed towards a more fundamental understanding of the effect of the different promoter elements on the catalytically active Co particles. Due to the extensive open and patent literature, we have mainly included research publications of the last two decades in our review paper.<sup>43–177</sup> In addition, we will limit ourselves to catalyst formulations composed of oxide supports, excluding the use of other interesting and promising support materials, such as, *e.g.*, carbon nanofibers studied by the group of de Jong.<sup>178,179</sup>

The paper starts with an introduction in F–T catalysis, including some recent developments in gas-to-liquid technologies and an overview of the main F–T catalyst compositions. In a second part, we will focus on the effect of promoter

elements on Co-based F–T catalysis. A classification for the different modes of promotion effects will be proposed and each promoter element reported in literature will be accordingly evaluated. The obtained insights have led to guidelines to design improved Co-based F–T catalysts. A third part will deal with some highlights on the literature of Mn-promoted F–T catalysts and a comparison between supported and unsupported Mn-promoted Fe-, Ru- and Co-based F–T catalysts will be made. It will be shown that many advanced characterization techniques, including spectroscopy and microscopy, are necessary to reveal physicochemical insights in this complex catalytic system. The paper ends with some concluding remarks and a look into the future.

## 2 Fischer–Tropsch Catalysis

### 2.1 Gas-to-Liquid Technology, Economic Impact and its Relevance to Society.

– At present, the main commercial interest in F–T is the production of high quality sulfur-free synthetic diesel fuels from natural gas, currently being flared at crude oil production wells.<sup>21–27</sup> This renewed interest in F–T synthesis has not just only come about as a result of the abundant supply of natural gas, but also because of the global development of fuel supplies and environmental regulations to improve air quality in cities around the world. While the concept of a hydrogen fuel economy remains an important option for the more distant future, synthetic diesel is being promoted by the fuel industry as the most viable next step towards the creation of a sustainable transport industry. Some advantages of synthetic diesel are:

- Low content of sulphur and aromatic compounds
- High cetane number
- Low particulate formation
- Low NO<sub>x</sub> and CO emission

At the same time, increased efficiencies in the F–T process and the ability – based on past experience – to build large-scale plants to capture the economies of scale have made the F–T gas-to-liquid (GTL) technology attractive and competitive with the current crude oil refinery industries.

It has been estimated that F–T GTL should be viable at crude oil prices of about \$20 per barrel. For some time now the oil price has been well above \$50 per barrel (more recently it has even topped above \$70 per barrel), making it a very appealing technology for countries, having huge reserves of natural gas, but little local market for it and no major pipeline infrastructure to ship it to larger economies. Alternatively, such countries could crack ethane or propane to make ethylene or propylene and further convert it into polyethylene or polypropylene, which can then be shipped to more heavily populated areas in the world. All this holds for the Middle East countries and, *e.g.*, Saudi Arabia is known to heavily invest in propane dehydrogenation plants and polypropylene production facilities, while Qatar is focusing on F–T GTL activities. These activities are concentrated near Ras Laffan in Qatar's northern gas field,

holding 9% of the world's proven gas resources.<sup>25</sup> Table 1 gives a summary of the currently operated and recently announced F–T plants based on natural gas, together with the expected production levels and the industrial companies and countries involved.<sup>21–23,26</sup> Industry projections suggest that by 2020 the total GTL capacity in the world could reach more than  $1 \times 10^6$  bpd.

Currently, there are two F–T plants operating on offshore methane. The first one is the Shell Bintuli plant in Malaysia, which produces 15000 barrels per day. The second one is the Moss Bay plant (PetroSA) located in South Africa. Recently, Sasol/Chevron, ExxonMobil and Shell announced major investments in F–T GTL plants.<sup>21–23</sup> In addition, there are many small (mainly for local markets) and large (mainly for export) project proposals for F–T GTL projects on the table. Most of the large project proposals are in the Middle East

**Table 1** *Currently operating and recently announced F–T plants based on methane, together with the industrial companies and countries involved, the used Co F–T catalyst technology, the (expected) production levels and the (expected) year of start-up (barrels per day, bpd)*

Country	Company or companies	Technology	Production level (bpd)	Start-up year
South-Africa	PetroSA	Sasol's slurry phase technology	20 000	1992
Malaysia	Shell	Shell middle distillate synthesis (SMDS) fixed-bed technology	15 000	1993
Qatar	Sasol and Qatar Petroleum, in alliance with Chevron	Sasol's slurry phase technology	34 000	2005 (2 other F–T plants are scheduled to operate in the coming years with the second F–T plant having a scale of 65 000 bpd)
Nigeria	Chevron Nigeria (Sasol/Chevron alliance) and Nigeria National Petroleum Company	Sasol's slurry phase technology	34 000	2007
Qatar	Shell and Qatar Petroleum	Shell middle distillate synthesis (SMDS) fixed-bed technology	140 000	2009 (first train of 70 000 bpd)/2010 (second train of 70 000 bpd)
Qatar	ExxonMobil and Qatar Petroleum	Advanced gas conversion for the 21st century (AGC-21) technology	154 000	2011

(Qatar), while the other envisaged projects are in Russia, Australia, Argentina, Egypt, Iran, Bolivia, Brazil, Indonesia, Malaysia and Trinidad. Especially, Russia is expected to have significant long-term potential for F–T GTL technology taking into account the huge country's gas reserves.

**2.2 Fischer–Tropsch Catalysts.** – It is well known that all Group VIII transition metals are active for F–T synthesis. However, the only F–T catalysts, which have sufficient CO hydrogenation activity for commercial application, are composed of Ni, Co, Fe or Ru as the active metal phase. These metals are orders-of-magnitude more active than the other Group VIII metals and some characteristics of Ni-, Fe-, Co- and Ru-based F–T catalysts are summarized in Table 2.

The exact choice of the active F–T metal to be used in a particular catalyst formulation depends on a number of parameters, including the source of carbon used for making syngas, the price of the active element and the end products wanted. F–T catalysts for the conversion of syngas made from a carbon-rich source, such as coal, are usually based on Fe. This is due to the high WGS activity of Fe, as given in reaction (2), so that less hydrogen is required and oxygen exits the reactor in the form of carbon dioxide. There are, however, new environmental considerations such as the greenhouse effect, which may preclude the future use of Fe precisely due to its high WGS activity. In the case of syngas production from hydrogen-rich carbon sources, such as natural gas, the preferred catalysts due to their lower WGS activities are based on Co or Ru.

Nickel F–T catalysts, due to an easy dissociation of CO, possess too much hydrogenation activity, unfortunately, resulting in high yields of methane. At elevated pressure, Ni tends to form nickel carbonyl compounds (highly toxic), and the active component of the catalyst is lost from the F–T reactor. In addition, with increasing reaction temperature the selectivity changes to mainly methane with Ni. This tendency is also observed with Co- and Ru-based catalysts. Instead, with Fe, the selectivity towards methane remains low even at high reaction temperatures. Ru is the most active F–T element working at the lowest reaction temperature of, *e.g.*, only 150°C, very high molecular weight products have been isolated. However, the very low availability and as a consequence the high cost of Ru makes the use of this element in large-scale industrial F–T applications questionable.

This leaves Co and Fe as the most appropriate elements to prepare commercially interesting F–T catalysts and both systems have their own advantages

**Table 2** Overview of some characteristics of Ni-, Fe-, Co- and Ru-based F–T catalysts

<i>Active metal</i>	<i>Price</i>	<i>F–T activity</i>	<i>WGS activity</i>	<i>Hydrogenation activity</i>
Ni	++++	+	+/-	+++++
Fe	+	+	+++	+
Co	+++	+++	+/-	+++
Ru	+++++	+++++	+/-	+++



and disadvantages. It is important to notice that Co is 3 times more active than Fe in F–T while its price is over 250 times more expensive. Because of the relatively low cost of Fe, fresh catalyst material can be added on-line to fluidized bed reactors, and this practice results in long runs at high conversion levels. This luxury cannot be afforded for the more expensive Co F–T catalysts and so, it is vital that the minimum amount of Co is employed, while maintaining its high activity and long effective catalyst life. Co-based catalysts are preferred for the production of paraffins, as they give the highest yields for high molecular weight hydrocarbons from a relatively clean feedstock, and produce much less oxygenates than Fe catalysts. This is due to a higher hydrogenation activity of Co compared to Fe. On the other hand, if linear olefins are wanted as the end product, it is better to employ Fe-based F–T catalysts because there is less secondary hydrogenation of the primary formed olefins. However, Fe-based catalysts are known to produce aromatics and other non-paraffins, such as oxygenated compounds, as by-products.

Another difference between Co and Fe is their sensitivity towards impurities in the gas feed, such as H<sub>2</sub>S. In this respect, Fe-based catalysts have been shown to be more sulfur-resistance than their Co-based counterparts. This is also the reason why for Co F–T catalysts it is recommended to use a sulphur-free gas feed. For this purpose, a zinc oxide bed is included prior to the fixed bed reactor in the Shell plant in Malaysia to guarantee effective sulphur removal. Co and Fe F–T catalysts also differ in their stability. For instance, Co-based F–T systems are known to be more resistant towards oxidation and more stable against deactivation by water, an important by-product of the FTS reaction (reaction (1)). Nevertheless, the oxidation of cobalt with the product water has been postulated to be a major cause for deactivation of supported cobalt catalysts. Although, the oxidation of bulk metallic cobalt is (under realistic F–T conditions) not feasible, small cobalt nanoparticles could be prone to such reoxidation processes.

### 3 Co-based Fischer–Tropsch Catalysts

While there have been much activity in the literature addressing Fe, Ru and Ni F–T catalysts, the largest body of papers and patents in the last three decades have dealt with Co-based F–T catalysts in attempts to make more active catalysts with high wax selectivities. It is, however, remarkable to notice that modern Co F–T catalysts are still very similar to the ones prepared by Fischer and co-workers; *i.e.*, they consist of promoted cobalt particles supported on a metal oxide and most of, if not all, Co-based F–T catalyst compositions contain the following components:

- (i) Co as the primary F–T metal;
- (ii) A promoter metal, possessing noble metal behavior, *e.g.*, Ru, Re, Pd, Pt, Rh and Ir. The main function of this promoter element is to facilitate the reduction of the cobalt nanoparticles; and as a consequence to increase the

- number of active cobalt sites. As will be shown later these promoters have also other beneficial effects on the catalyst performance;
- (iii) An oxidic promoter elements, such as lanthanide and thorium oxide, ceria, zirconia, titania, vanadia, chromia and manganese oxides. However, their roles are much broader; and
  - (iv) A high surface area oxide support, mostly alumina, titania and silica, although the use of supports such as ceria, zirconia, magnesia, gallia, silica-alumina, zeolites (*e.g.* zeolite Y, silicalite, ZSM-5 and ETS-10), ordered mesoporous oxides (*e.g.* MCM- and SBA-type materials having high surface area and a narrow pore-size distribution) and delaminated zeolites (*e.g.* ITQ-2 and ITQ-6) are also reported in literature.<sup>180–190</sup>

The role of the support material is rather well established. It provides mechanical strength and thermal stability to the Co nanoparticles, while facilitating a high Co dispersion. The choice of the support oxide largely determines the number of active Co metal sites stabilized after reduction, as well as the percentage of supported cobalt oxides that can be reduced to cobalt metal. This is due to a different Co-support oxide interaction. A strong Co-support oxide interaction, as it occurs in the case of alumina and titania, favors the dispersion of the supported Co particles, but at the same time decreases their reducibility, leading to catalyst materials with a limited number of accessible surface Co metal sites. On the contrary, a much weaker interaction leading to a higher Co reducibility occurs for Co/SiO<sub>2</sub> catalysts. In this case, the cobalt particles tend to agglomerate on the support surface during the thermal activation treatments resulting in a relatively low Co dispersion, and thus a low number of surface Co metal sites. Recent studies with ordered mesoporous oxides have shown that cobalt particles with defined particle sizes by confinement within the mesoporous channels are active for F–T catalysis.<sup>180–190</sup> An increase of the average particle size of the supported Co particles was found with increasing pore size of the mesopores silica; these larger particles are more reducible and lead to catalyst materials with higher F–T activity. Similar effects have been observed for Co/SiO<sub>2</sub> catalysts made from commercial amorphous silicas with increasing pore diameters.<sup>191</sup>

On the other hand, the origin of the promoter metal and metal oxide effects is not always clear, despite the many detailed characterization studies. In what follows, we will give first a possible definition of the different promotion phenomena described in literature, as well as their mode of operation. The second part deals with an extensive literature overview of the effect of each promoter element on the F–T activity, selectivity and stability of the active Co phase. The different modes of operation will be evaluated for each element. Special attention will be paid to noble metal and transition metal oxide promotion effects.

**3.1 Promotion Effects.** – The catalyst surface often contains substances that are added deliberately to modify the turnover rate for a given catalytic reaction.<sup>191–194</sup> The simplest case being an additive that increases the rate per

site per second. It is, in this respect, useful to recall the concepts of catalyst promotion. Promoters are doping agents added to catalyst materials in small amounts to improve their activity, selectivity and/or stability.<sup>30</sup> It is generally accepted that promoter elements may induce these beneficial effects in several manners. All this has led researchers to come up with a classification scheme for promoter effects and in the case of the Co F–T literature the following names (including often different definitions!) have been given to the different types of promotion: structural or structure promoters, electronic promoters, textural promoters, stabilizers and catalyst-poison-resistant promoters. Since many of the above-mentioned effects tend to overlap in practice, it is sometimes difficult to precisely define the observed function of a promoter. In addition, the degree to which additives modify a catalyst's activity in the positive or negative manner is also dependent on the amount of the additive, the support oxide under consideration and the exact preparation method, causing them to act either as a promoter or a poison. In line with this reasoning, the term modifier should be more appropriate according to Paal and Somorjai.<sup>190</sup> Finally, it is important to mention that promoter elements are mostly discovered in a serendipitous manner and this holds most probably also for the field of Co F–T catalysis. Only a few of them are expected to be the result of *a priori* catalyst design.

In this review paper we have chosen to divide the family of promoter elements into two classes according to their intended function. *Structural promoters* affect the formation and stability of the active phase of a catalyst material, whereas *electronic promoters* directly affect the elementary steps involved in each turnover on the catalyst. The latter group of promoters affect the local electronic structure of an active metal mostly by adding or withdrawing electron density near the Fermi level in the valence band of the metal. This results in a modification of the chemisorption properties of the active metal. Hence, this affects the surface coverage of reactants and, as a consequence, the catalysis done by the metal. In addition to these two groups of promoters we have included in our classification the group of synergistic promotion effects. Although promoter elements are not considered themselves to be catalytically active, they may play other roles under F–T conditions. This may indirectly affect the behaviour of the catalytic active element, still dominating the overall catalytic performances of the catalyst material. We will now discuss more in detail the different promoter effects encountered in Co F–T catalysis.

**3.1.1 Structural Promoters.** The main functions of structural promoters are to influence the cobalt dispersion by governing the cobalt-support oxide interaction.<sup>30</sup> A high Co dispersion results in a highly active Co metal surface and, therefore, in a high coverage by the reactants, and as a consequence an improved catalyst activity. Structural promotion may lead to an increased catalyst activity and stability, but in principle does not influence the product selectivity since it only increases the number of active sites in a catalyst material. This increase in active sites can be achieved by a stabilization of the

Co active phase due to the promoter element, which either avoids the formation of metal-support compounds, or prevents the agglomeration and sintering of the Co particles under F–T operation conditions.

*3.1.1.1 Stabilizing the Support Oxide.* Promoter elements can be added to the support oxide resulting in a decreased Co compound formation with the support oxide. This is illustrated in Figure 3A. More specifically, strategies should be followed to avoid the formation of either cobalt titanate, cobalt silicate or cobalt aluminate as a result of Co solid-state diffusion under reducing or regeneration conditions in the subsurface of these support oxides. Some transition metals, for example Zr or La, could act in such a way.

A related problem is the reduction in support surface area. This is especially a problem in the case of titania, where the anatase polymorph is only stable under oxidative regeneration conditions from about 400°C to 750°C. The addition of Si, Zr and Ta as promoter elements may avoid or diminish surface collapse of the support oxide.

*3.1.1.2 Glueing the cobalt particles on the support oxide.* Some promoter elements can act as an oxidic interface between the supported Co particle and the support oxide, leading to an increased stability of the cobalt particles against sintering during reduction or oxidative regeneration. A plausible schematic representation of this promotion effect is shown in Figure 3B.

*3.1.1.3 Promoters leading to increased cobalt dispersion.* The addition of promoter elements may also lead to increased cobalt dispersion after preparation. In the absence of the promoters, relatively large cobalt crystals are formed, whereas, by adding these additives, smaller supported cobalt particles can be made. Such promotion effect is illustrated in Figure 3C.

Related to this effect it is important to mention that small metal particles composed of a promoter element can dissociate hydrogen in the neighbourhood of a supported cobalt particle leading to the formation of atomic hydrogen that may spill over by diffusion to cobalt,<sup>30</sup> as illustrated in Figure 3D. This can result in an enhanced degree of cobalt reduction and therefore a higher amount of surface cobalt metal atoms. The result of this promotion is an increase in the number of active sites and therefore a higher catalyst activity, leaving the catalyst selectivity unaltered. Noble metals, such as Re, Pt and Ru, are known to act in this manner.

*3.1.2 Electronic Promoters.* In contrast to structural promoters, electronic effects are much less obvious to be detected in an unambiguous manner. Electronic promotion can be best understood in terms of ligand effects. The surrounding (electronic) environment of an active Co site can be altered by the presence of a promoter element. This leads to an electronic donation or withdrawal leading to an increased intrinsic turnover frequency or change in product selectivity. Ligand effects may also result in a decreased deactivation rate by altering the adsorption/desorption properties of the reagents/reaction products. Electronic promotion can only occur when there is a direct chemical

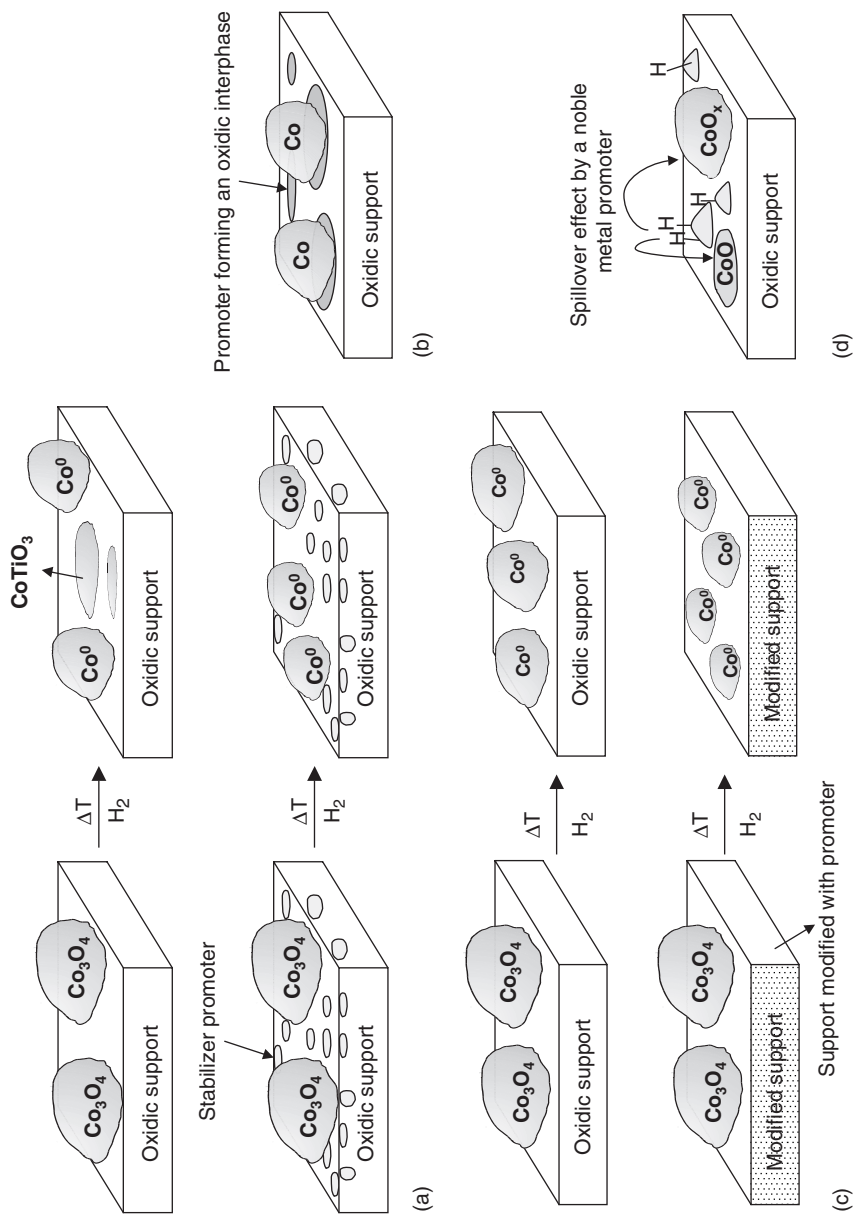


**Figure 3** The different modes of action of structural promoters in Co-based Fischer–Tropsch catalysis: (a) structural promoter elements can lead to a decreased Co compound formation with the support oxide; (b) structural promoter elements can act as an oxidic interface between the supported Co particle and the support oxide; (c) structural promoter elements may lead to an increased cobalt dispersion; and (d)  $\text{H}_2$  spillover effect, leading indirectly to a higher dispersion of the supported Co particles

interaction between the promoter element and the cobalt active surface. It is important to mention that electronic metal-support effects have been found to exist in heterogeneous catalysis, but these effects should only play a minor role in Co F–T catalysis since the active Co particles are relatively large and the contact area between support and cobalt particle is therefore very small. Finally, electronic effects induced by promoter elements may be responsible for an increased resistance of the supported Co nanoparticles to re-oxidation or even their stability against deactivation in general.

**3.1.2.1 Promoter metal oxide decoration of the cobalt surface.** A first way to induce a ligand effect is to decorate the active cobalt surface with metal oxides. In this way, the catalyst surface properties are altered, resulting in improved selectivities and/or activities. It should be clear that a beneficial catalytic effect can only be obtained if the deposited metal oxides are not blocking (all) the active cobalt sites, which would lead to a decreasing hydrogen or CO chemisorption. The decoration effect of a supported Co particle by transition metal oxides is illustrated in Figure 4A. A similar effect may occur with the support oxide as decorating material. This effect is generally known as the “strong metal-support interaction” or SMSI effect.<sup>30,195</sup> The SMSI effect is explained in Figure 4B. When metals supported on, *e.g.*, titania are heated in hydrogen at relatively high temperatures, a dramatic decrease in hydrogen and CO chemisorption occurs. This observation is due to a partial encapsulation of the supported metal particle by the support oxide since reduced  $\text{TiO}_x$  ensembles can migrate over the metal surface, leading to a (partial) decoration of the metal particle.

**3.1.2.2 Cobalt-promoter alloy formation.** Metal alloying or bimetallic alloy formation may also influence the activity and selectivity of Co F–T catalysts.

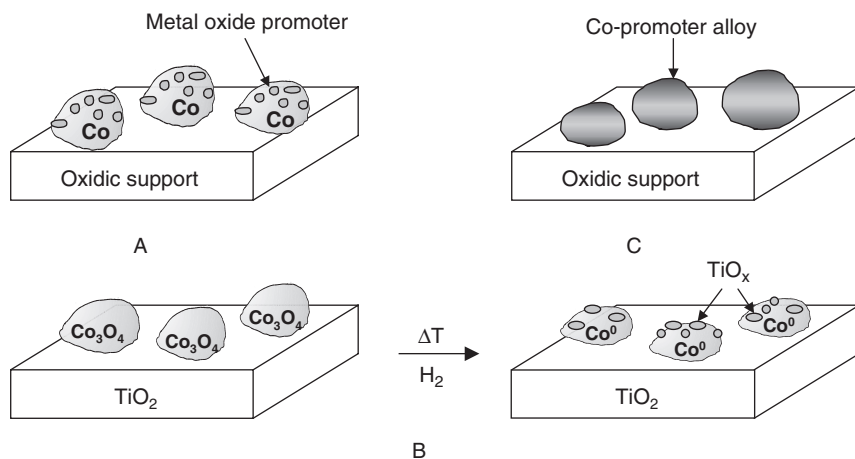


**Figure 4** The different modes of action of electronic promoters in Co-based Fischer–Tropsch catalysis: (A) promoter metal oxide decoration of the cobalt surface; (B) the SMSI effect; and (C) cobalt-promoter alloy formation

Indeed, cobalt and a promoter metal may form an integral metal particle deposited on the support oxide, altering the electronic properties of the surface cobalt metal atoms (Figure 4C). Depending on the promoter element added to the Co cluster, alloying might lead to an increased catalyst activity, selectivity, as well as stability.

**3.1.3 Synergistic Promotion Effects.** As was already mentioned promoter elements are not considered themselves to be catalytically active, but it is fair to say that this is not always the case. This promoter activity may indirectly affect the behaviour of the catalytic active element since it will alter, *e.g.*, the local feed composition or may, due to its catalytic properties, influence the overall reaction product distribution. The following effects, illustrated in Figure 5, are expected to occur in a promoted Co F–T catalyst.

**3.1.3.1 Water-gas shift reaction.** The water-gas shift (WGS) reaction (reaction (2)) made by particles composed of a promoter element close to a supported cobalt particle leads to a change in the local CO/H<sub>2</sub> ratio, which may affect the surface coverage of cobalt. As a result, both the activity and the selectivity of the catalyst can be altered. Some transition metal oxides are known to act as WGS reagents.

**3.1.3.2 Hydrogenation/dehydrogenation reactions.** The end products of the F–T process are a mixture of higher alkanes and alkenes. The promoter elements could show under F–T conditions some activities for hydrogenation or dehydrogenation reactions leading to a shift in the relative ratio of alkanes to alkenes.

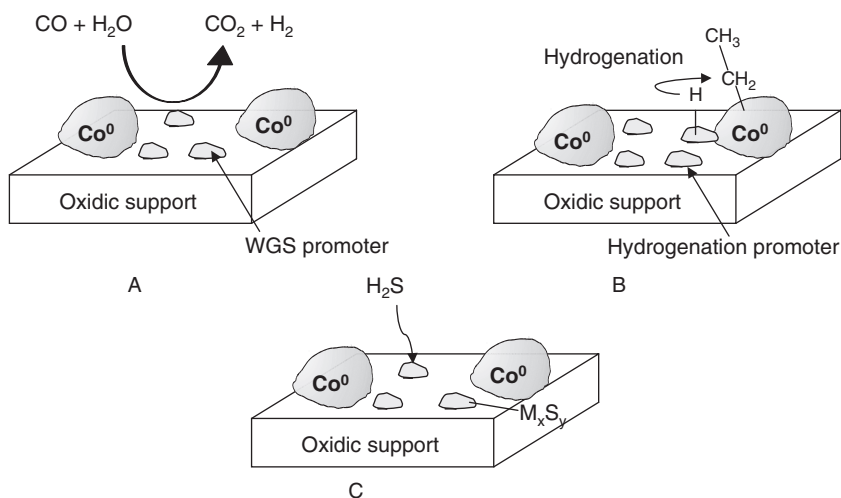


**Figure 5** Survey of possible synergistic promotion effects occurring in Co-based Fischer–Tropsch catalysis: (A) water-gas shift reaction, (B) hydrogenation/dehydrogenation reactions; and (C) H<sub>2</sub>S adsorption

3.1.3.3 *Coke burning during regeneration.* Co F–T catalysts deactivate due to coke formation blocking the active sites. This coke can be burned off by an oxidative treatment. The addition of promoter elements may decrease the temperature of this oxidative treatment, preventing the possible clustering of supported cobalt particles.

3.1.3.4 *H<sub>2</sub>S adsorption reaction.* As was already mentioned, Co F–T catalysts are prone to H<sub>2</sub>S poisoning and the addition of specific promoter elements may lead to an increased H<sub>2</sub>S tolerance. Crucial for this are the use of promoter elements, such as B and Zn, which make stable surface compounds with sulfur.

**3.2 Overview of the Promoter Elements Used in Co-based F–T Catalysts.** – The following chemical elements have been investigated as promoters in Co-based F–T catalysis: B, Mg, K, Ti, V, Cr, Mn, Ni, Cu, Zr, Nb, Mo, Ru, Rh, Pd, La, Re, Ir, Pt, Ce, Gd and Th.<sup>43–177,247–261</sup> Taking the above described classification scheme, we have made an attempt to identify for every reported promoter element its beneficial effect for Co F–T catalysis. The result of this effort is summarized in Table 3. It is clear from this table that different promoter elements could have multiple modes of promotion action. Furthermore, in making this table we encountered several research papers giving opposite

**Table 3** Overview of the promotion effects of different elements used in literature on the Co F–T catalyst performances

Promotion type	Influence on catalyst			Element reported in literature to play a role in this promotion effect	
	Promotion mode	Activity	Selectivity		Stability
Structural	Support stabilization	+		+	Mg, Si, Zr, Nb, Rh, La, Ta, Re, Pt
	Cobalt glueing	+		+	B, Mg, Zr
	Cobalt dispersion increase	+		+	Ti, Cr, Mn, Zr, Mo, Ru, Rh, Pd, Ce, Re, Ir, Pt, Th
Electronic	Decorating cobalt surface	+	+	+	B, Mg, K, Ti, V, Cr, Mn, Zr, Mo, La, Ce, Gd, Th
	Cobalt alloying	+	+	+	Ni, Cu, Ru, Pd, Ir, Pt, Re
Synergistic	Watergas shift	+	+		B, Mn, Cu, Ce
	Hydrogenation/dehydrogenation		+		nr <sup>a</sup>
	Coke burning			+	Ni, Zr, Gd
	H <sub>2</sub> S adsorption			+	B, Mn, Zn, Zr, Mo

<sup>a</sup> One may anticipate that hydrogenation and dehydrogenation reactions can be catalyzed by metals and metal oxides known to be active for this reaction. Examples are CrO<sub>x</sub> and Pt.



conclusions on the observed promotion effect. Such differences can only be explained by the different loadings and preparation methods employed in making the promoted Co F–T catalysts, as well as different F–T reaction conditions employed, leading to different conversions and selectivities. In what follows, we discuss some highlights of noble metal and transition metal oxide promotion of Co-based F–T catalysts.

**3.2.1 Noble Metal Promotion Effects.** In the group of noble metals; Ru, Re and Pt have been extensively studied as promoter elements for Co-based F–T catalysts, whereas other metals, such as Rh, Pd, Os and Ir, are only reported in limited occasions. Hence, we will focus our attention on the promotion effects induced by Ru, Re and Pt.

**3.2.1.1 Ruthenium.** Ru is the most studied noble metal promoter and it has been frequently showed to play a role both in structural and electronic promotion.<sup>43–84,146,149,155,157,160–168,170,174,176,177,254,260</sup> In the early nineties, Turney *et al.* observed that the addition of Ru to Co/CeO<sub>2</sub> catalysts drastically increased the Co F–T activity without modifying the catalyst selectivity.<sup>44,45</sup> Results obtained from XPS and TPR indicated that Ru caused a decrease of the reduction temperature of supported Co<sub>3</sub>O<sub>4</sub> nanoparticles. The authors proposed that Ru facilitates the reduction of cobalt via a hydrogen spillover from Ru to Co, thereby leading to an increase of the number of exposed Co<sup>0</sup> sites and consequently, to an increase in the CO hydrogenation rate. This structural promotion of Ru has been shown to take place independently of the support material; *i.e.*, the addition of Ru to Co/Al<sub>2</sub>O<sub>3</sub>,<sup>49</sup> Co/SiO<sub>2</sub><sup>157</sup> and Co/TiO<sub>2</sub><sup>46</sup> catalysts decreases the temperature at which CoO<sub>x</sub> is reduced to Co<sup>0</sup> during activation, leading to catalysts with improved cobalt dispersions.

The role of Ru as an electronic promoter has also been extensively investigated. In this respect, it is worthwhile to point out that Co–Ru catalysts exhibit exceptional high selectivities to C<sub>5+</sub> products and higher turnover rates compared to unpromoted Co catalysts.<sup>146</sup> A remarkable insight into Ru promotion has been gained from the work of Iglesia *et al.*<sup>43,46</sup> This group observed that at reaction conditions that favor the formation of higher hydrocarbons (*i.e.*, high pressures and high conversions), the apparent turnover numbers on cobalt catalysts are independent of the support material, but are markedly increased by the addition of small amounts of Ru. They found large increases in the turnover rates and the C<sub>5+</sub> selectivity when Ru was added to Co/TiO<sub>2</sub> catalysts in a ratio of Ru/Co < 0.008.<sup>46</sup> The experimental results indicated that Ru inhibits the deactivation of the catalysts by keeping the Co surface “clean” and hence, preventing a carbon deposition on the Co particles. This promotion appeared to require an intimate contact between Co and Ru atoms, since a bimetallic nature of the active sites was found to exist and this nature was enhanced by oxidation treatments at high temperatures (> 573 K). On the other hand, the higher C<sub>5+</sub> selectivities found for the Ru-promoted catalysts were discussed in terms of an increase in the Co site density. Apparently, a higher Co

site density inherent in the Co–Ru catalysts leads to diffusion-enhanced re-adsorption of  $\alpha$ -olefins, which reverses the  $\beta$ -hydrogen abstraction termination step and thus, favors the formation of higher hydrocarbons.<sup>53</sup>

Many other groups have recently reported on the effects of Ru promoter in the performances of Co F–T catalysts. For example, Sun *et al.* observed that the addition of small amounts of Ru to Co/SiO<sub>2</sub> catalysts increased the TOF, whereas it did not affect the CH<sub>4</sub> selectivity.<sup>69</sup> Ru appeared to be enriched at the metallic cobalt surface after reduction, modifying the adsorption properties of the Co<sup>0</sup> sites. Price *et al.* investigated Co/TiO<sub>2</sub> and Co–Ru/TiO<sub>2</sub> catalysts with infrared (IR) spectroscopy making use of CO as a probe molecule.<sup>52</sup> They concluded that their Ru–Co and Co catalysts had different surface structures and confirmed the existence of Co–Ru interactions. Finally, Hosseini *et al.* investigated the effect of Ru loading on a 20 wt% Co/Al<sub>2</sub>O<sub>3</sub> catalyst,<sup>81</sup> and observed that Ru promotion was only achieved for Ru loadings of 0.5 and 1.0 wt%. Higher Ru loading of 1.5 and 2.0 wt% led, however, to a decrease in the CO hydrogenation activity. On the other hand, the C<sub>5+</sub> selectivity remained almost unaffected by the Ru loading.

**3.2.1.2 Rhenium.** Re promotion has also been widely investigated in Co-based F–T catalysis.<sup>85–98,153,168,171,174,177,253</sup> Re is regarded as a structural promoter and it has been frequently reported to increase the Co reducibility *via* a hydrogen spillover effect, leading to catalysts with enhanced Co dispersions. Re reduces to a metallic state at higher temperatures than Ru and therefore, can facilitate the second cobalt reduction step, from CoO to Co<sup>0</sup>.<sup>96</sup>

Hilmen *et al.* performed TPR experiments on Co/Al<sub>2</sub>O<sub>3</sub> and Co–Re/Al<sub>2</sub>O<sub>3</sub> catalysts, and on physical mixtures of Co/Al<sub>2</sub>O<sub>3</sub> and Re/Al<sub>2</sub>O<sub>3</sub>, and they suggested that no direct contact between Re and Co is necessary to achieve the promotion by Re.<sup>86</sup> Hence, Re might be in many cases located on the support material rather than decorating the surface of Co. In line with the above reasoning, Rygh *et al.* showed with DRIFTS studies that the presence of Re on Co/Al<sub>2</sub>O<sub>3</sub> catalysts increased the amount of bridged CO-adsorbed species without any sign of electronic interaction between the two metals.<sup>89</sup> Moreover, the oxidation or hydrogenation revealed bands arising from Re carbonyl species, suggesting that the Re was located at the catalyst surface. Nonetheless, other authors have reported the existence of bimetallic interactions between Co and Re. For example, Bazin *et al.* investigated the effect of Re on the structure of Re–Co/Al<sub>2</sub>O<sub>3</sub> catalysts by EXAFS<sup>94</sup> and the analysis of the Co K edge and Re L<sub>III</sub> edge provided direct evidence for Re–Co bond formation. Their results suggest that Re prevents the formation of cobalt surface phases, such as cobalt aluminate, resulting in an increase of the catalyst activity. They also considered that Re prevents the agglomeration of small metal particles in oxidizing environments and thus their migration and sintering. In another paper, Ronning *et al.* showed from the Re L<sub>III</sub> edge that small bimetallic particles were formed after reduction of Co–Re/Al<sub>2</sub>O<sub>3</sub> catalysts containing 4.6 wt% Co and 2 wt% Re.<sup>91</sup> More recently, Jacobs *et al.* have reported EXAFS data on Co–Re/Al<sub>2</sub>O<sub>3</sub> systems.<sup>96</sup> They proposed that a direct

contact of Re with the Co atoms existed, while evidence for Re–Re bonds was not observed. In addition, they observed that the average Co cluster size decreased with increasing Re loading.

It is generally believed that the addition of Re to Co-based catalysts leads to an increase in the F–T activity as a result of the increased number of exposed sites, although the intrinsic activity of the Co sites is not expected to change. For instance, Li *et al.* showed that the addition of 0.34 wt% Re to Co/TiO<sub>2</sub> catalysts with 10 wt% Co, resulted in the highest F–T conversion compared to unpromoted and Ru-promoted Co/TiO<sub>2</sub> catalysts.<sup>168</sup> On the other hand, the selectivity of the Co sites is generally expected to be not directly affected by the presence of Re,<sup>153</sup> although some authors have reported improvements in the C<sub>5+</sub> selectivity when using Re.<sup>94,171</sup> A possible explanation may be the influence of Re on the Co particle sizes distribution, which may also have an indirect effect on the selectivity due to the changes in the Co surface density. Some differences found in literature may also arise from comparisons of the catalysts at different conversions, which lead to significant variations in selectivities.

**3.2.1.3 Platinum.** Pt is another noble metal considered to play a role as structural promoter, and it is frequently reported to enhance the Co dispersion in supported Co F–T catalysts.<sup>99–108,150,153,160,162,164,166,167,176,177,258,260,261</sup> In the early nineties, Zsoldos *et al.* reported XPS results on Pt-promoted Co/Al<sub>2</sub>O<sub>3</sub> catalysts, in which the Co reducibility was largely improved when combined with small amounts of Pt.<sup>99</sup> They observed that the highly dispersed, but difficult to reduce surface cobalt particles were largely reduced in the Pt–Co/Al<sub>2</sub>O<sub>3</sub> catalyst, whereas only the larger Co<sub>3</sub>O<sub>4</sub> particles were reduced in the Co/Al<sub>2</sub>O<sub>3</sub> catalyst. It was suggested that Pt would prevent the formation of Co aluminates during catalyst preparation and that the Pt might partially cover the surface of the Co metal and even form bimetallic Pt–Co particles. These findings were further evidenced in two following papers.<sup>100,101</sup> A year later, Zsoldos and co-workers showed using XPS that Pt–Co/Al<sub>2</sub>O<sub>3</sub> catalysts with a high Pt/Co ratio (Co atomic fraction of 0.2–0.5) contained CoPt<sub>3</sub> bimetallic particles at the surface of the Co nanoparticles.<sup>102</sup> The existence of Co–Pt interactions in these catalytic systems was further confirmed by Tang *et al.* making use of IR with CO as probe molecule.<sup>104</sup> The results suggested that there was a strong interaction between Pt and Co atoms. Very recently, Jacobs *et al.* have reported on Co–Pt/Al<sub>2</sub>O<sub>3</sub> catalysts investigated by EXAFS at the Pt L-edge, and they concluded that isolated Pt atoms interact with the supported cobalt clusters without forming Pt–Pt bonds.<sup>107</sup> The Co K-edge was used to verify that the cobalt cluster size increased slightly for those systems with Pt promotion, in which the cobalt reduction extent increased by a factor of two and the formation of Co aluminates was prevented.

Pt promotion has been also investigated with other support materials. For example, Schanke *et al.* studied the influence of small amounts of Pt (0.4 wt%), on the reducibility of Co/SiO<sub>2</sub> and Co/Al<sub>2</sub>O<sub>3</sub> catalysts containing 9 wt% Co, and observed that the presence of Pt decreased in all cases the reduction temperature of Co<sub>3</sub>O<sub>4</sub>, although the effect was more pronounced for

alumina-supported Co F–T catalyst.<sup>103</sup> In this work the CO hydrogenation rates at pressures of 1 bar were found to be 3–5 times higher in the Pt-promoted catalysts than in the unpromoted counterparts. However, steady state and transient kinetic experiments indicated constant turnover frequencies for CO hydrogenation in all catalysts, independent of the support or the presence of Pt. Thus, the higher apparent turnover numbers for the Pt-promoted catalysts were considered to be due to a higher coverage of intermediates and not by an increase in the intrinsic activity. In addition, the F–T selectivity was not influenced by the presence of Pt. Similar findings were reported by Vada *et al.* They observed that the addition of 1 wt% Pt to a Co/Al<sub>2</sub>O<sub>3</sub> catalyst containing 8.7 wt% Co, significantly increased the CO hydrogenation rate, whereas the selectivity was unaffected.<sup>153</sup> Hence, it was argued that Pt increases the cobalt reduction extent and therefore the CO hydrogenation rate, although the average Co site activity is not altered. Finally, Das *et al.* have reported on Pt-promoted Co/Al<sub>2</sub>O<sub>3</sub> catalysts with 25 wt% Co and have observed that Pt promotion does not alter the Co dispersion but increases the amount of Co reduced.<sup>258</sup> Both unpromoted and Pt-promoted catalysts were found to decline in activity at the same rate.

**3.2.2 Transition Metal Oxide Promotion Effects.** Many transition metal oxides have been investigated as potential promoters for Co-based F–T catalysts.<sup>120–139,143–145,147–149,151–152,154,158–161,165,166,168–173,251,252,255–259</sup> Although different promotion functions are proposed in the literature, mostly, transition metal oxides have been regarded as electronic promoters, having a direct influence on the intrinsic activity and/or selectivity of the Co sites. This effect is manifested through direct interaction of the supported cobalt particles with the transition metal oxides. Hence, the transition metal oxide promoters are thought to be spreading over the cobalt surface in submonolayer coverages, modifying the adsorption properties of the Co active sites. In this respect, it is worthwhile to highlight the work of Bartholomew *et al.*,<sup>118</sup> in which the activity of supported Co nanoparticles was compared with different oxide supports. The following decreasing order in activity was found: Co/TiO<sub>2</sub> > Co/SiO<sub>2</sub> > Co/Al<sub>2</sub>O<sub>3</sub> > Co/MgO. Since the Co dispersion was found to be very similar in the first three catalysts, the enhanced activity in the case of Co/TiO<sub>2</sub> appeared to be due to an electronic effect induced by the TiO<sub>2</sub>. This was attributed to the SMSI taking place with TiO<sub>2</sub>, as discussed in more detail before.

Early in the nineties Ruiz *et al.* reported enhanced catalyst activities and increased selectivities to alkenes and higher hydrocarbons upon addition of V, Mg, and Ce oxides to Co-based F–T catalysts.<sup>151</sup> These variations were attributed to electronic effects induced by the transition metal oxide. Similar results were obtained by Bessel *et al.* using a Cr promoter in Co/ZSM-5 catalysts.<sup>152</sup> This group observed that the addition of Cr improved the catalyst activity, and shifted the selectivity from methane to higher, generally more olefinic, hydrocarbons. Based on H<sub>2</sub> and CO chemisorption, as well as TPR and TPD results, they suggested that the promotion was caused by an interaction between the transition metal oxide and the cobalt oxide, which inhibits

cobalt reduction and improves Co dispersion. Furthermore, it was considered that Cr increased the Co–CO and decreased the Co–H bond strengths, resulting in a higher relative amount of CO/H absorbed on the Co particles. This effect would certainly lead to a lower hydrogenation rate during F–T synthesis. In other work, Kikuchi *et al.* reported the effect of Cr, Ti, Mn and Mo on the F–T performances of catalysts loaded with ultra fine Co particles.<sup>158</sup> The addition of these promoters effectively enhanced the catalyst activity, lowered the methane selectivity and increased the C<sub>5+</sub> production. They attributed these effects to a structural promotion, causing a decrease of the Co particle sizes in the catalysts. However, an electronic effect induced by the transition metal oxide promoters was not considered. Another promotion effect induced by Mn and Mo was reported by the group of Belosludov.<sup>169</sup> This group investigated the addition of Mn and Mo to Co-based F–T catalysts using computational chemistry. Interestingly, they found that the transition metal oxides under investigation improved the sulfur tolerance of the catalysts.

In recent years, some more detailed studies on transition metal oxide promotion have been reported. For example, Mendes *et al.* have reported on the promotion of Nb on Co/Al<sub>2</sub>O<sub>3</sub> catalysts, which were characterized using the temperature programmed surface reaction (TPSR) and diffuse reflectance spectroscopy (DRS) techniques.<sup>255</sup> The results showed a transient behaviour of the catalysts, being very well distinguished the catalyst containing Nb<sub>2</sub>O<sub>5</sub>. The authors proposed that an existent Co<sup>0</sup>–Co<sup>2+</sup> interface is responsible for the methanation reaction, whereas a Co<sup>0</sup>–NbO<sub>x</sub> is responsible for the hydrocarbon chain growth. The relative amount of each species on the surface was found to influence the selectivity of CO hydrogenation. Another recent study by Xiong *et al.* has reported on the F–T catalytic performances of Zr-modified Co/Al<sub>2</sub>O<sub>3</sub> catalysts.<sup>257</sup> The CoAl<sub>2</sub>O<sub>4</sub> spinel phase was detected in the prepared catalysts and its content decreased with increasing Zr loading. Thus, Zr appeared to inhibit the Co-support formation in the catalysts. Moreover, they observed improved activities and C<sub>5+</sub> selectivities upon the addition of Zr, and were attributed to the increase of the metal Co sites and reducibility. Similar results have been reported by Zhang *et al.* using a Mg promoter in Co/Al<sub>2</sub>O<sub>3</sub> catalysts.<sup>256</sup> They observed that the addition of Mg decreased the formation of a cobalt surface phase, which was detected by XPS. Small amounts of Mg were found to increase the catalyst activity by means of decreasing the formation of Co aluminates. However, large amounts of Mg caused a decrease in the reducibility of the catalysts due to the formation of MgO–CoO solid solutions.

#### 4 Mn-promoted Fischer–Tropsch Catalysts

We now discuss the main literature results on Mn-promotion for unsupported as well as supported Fe-, Ru-, and Co-based Fischer–Tropsch catalysts. Such comparison between Fe-, Ru- and Co-based catalysts has been shown to be very useful because it places the role of Mn as a promoter in F–T catalysis in a broader perspective.

**4.1 Mn-promoted Fe-based Fischer–Tropsch Catalysts.** – 4.1.1 *Unsupported Fe–Mn Fischer–Tropsch Catalysts.* Iron-based F–T catalysts possess both hydrogenation and WGS activity, imposing a flexible option as a working catalyst for typically coal-derived CO-rich syngas conversion. Iron-based catalysts often contain small amounts of K and some other metals/metal oxides as promoters to improve their activity and selectivity. Mn has been widely used as one of the promoters for unsupported Fe-based F–T catalysts, particularly in promoting the production of C<sub>2</sub>–C<sub>4</sub> olefins.<sup>196–205</sup>

Initially Mn was discovered to lower the methane selectivity and increase the olefin selectivity. More specifically, it was reported by Kolbel and Tillmetz<sup>196</sup> that “more than 50% Mn the remainder being Fe” or by Bussemeier *et al.*<sup>197,198</sup> “about equal parts of Fe and Mn” led to these beneficial F–T effects. In contrast to these results, van Dijk *et al.*<sup>199</sup> did not find any changes in the product formation when adding manganese oxide to an Fe F–T catalyst, although this work had been performed at atmospheric pressures, whereas the work of Kolbel and Tillmetz and Bussemeier was done at conditions close to industrial ones.

The findings of Bussemeier *et al.* and Kolbel and Tillmetz were, however, later on confirmed by the work of Barrault and co-workers<sup>199,200</sup> and a maximum increase in light olefin production was found for bulk chemical composition Fe/Mn ratios of 1. This group also explained the promotion effects in terms of electronic changes in the metal atoms by the surrounding manganese compounds; *i.e.*, an electronic promotion effect. On the other hand, Barrault *et al.* also concluded that the beneficial effect of the promoter was related to the preparation method used, and more specifically to the formation of specific Fe<sub>x</sub>Mn<sub>y</sub>O<sub>z</sub> precursor compounds. Other preparation routes were found to lead to other precursor species and, as a consequence, the final catalyst materials were also able to show less activity and selectivity. Calcination and reduction temperatures were found to be crucial in this respect. This important set of observations may explain the initial conflicting views on the promotion effect of Mn in Fe-based F–T catalysis.

In a series of seminal contributions by the group of Baerns it was reported that both the activity and selectivity of Fe-based F–T catalysts are affected by the addition of manganese oxides.<sup>201,202</sup> More specifically, the authors observed that (1) Mn-rich catalysts are rather resistant to deactivation; (2) the olefin to paraffin ratio is affected by the Mn content; the best selectivities towards olefins being obtained when Mn concentrations are about 15–20 wt%; (3) a reduction temperature of 400°C for the oxidic Mn–Fe catalyst precursors results in high initial activity, particularly for Fe-rich catalysts which then, however, deactivate rather severely as compared to when a 300°C reduction temperature is applied. The same authors also studied the changes in the catalyst materials after reduction and under conditions of Fischer–Tropsch synthesis. It was found that during reaction the catalyst material was transformed into Fe<sub>2</sub>MnO<sub>4</sub> and partly into the Fe<sub>5</sub>C<sub>2</sub> phase. Only minor amounts of Fe<sup>0</sup> could be detected during F–T synthesis. Years later, Bian *et al.* showed that the pre-reduction of the catalyst with CO or H<sub>2</sub> has a remarkable effect on the

catalyst performances.<sup>203</sup> This was explained in terms of different types of iron carbide species formed. CO-reduced catalysts exhibit remarkably higher catalytic activity for F–T synthesis than the H<sub>2</sub>-reduced catalysts. Furthermore, CO reduction was shown to be more effective for the formation of iron carbide (Fe<sub>x</sub>C).

The promotion effects of Mn on unsupported Fe-based F–T catalysts were also studied by Jensen and Massoth.<sup>204</sup> These authors concluded that the incorporation of Mn chemically and electronically promotes the active Fe surface. More particularly, it appears to alter the CO hydrogenation reaction path by suppressing the direct formation of paraffins from the reactive intermediate, leading to the increased production of higher olefins. Finally, Das *et al.* also observed that the addition of moderated amounts of Mn promoter to unsupported Fe F–T catalysts promotes the catalytic activity as well as the selectivity towards lower alkenes.<sup>205</sup>

Due to the importance of the Fe<sub>x</sub>Mn<sub>y</sub>O<sub>z</sub> precursor compounds to make true Mn-promoted Fe F–T catalysts, several groups have focused on the study of Fe, Mn-oxide compounds.<sup>206–210</sup> For example, Hearne and Pollak studied the coprecipitation of iron and manganese oxides, and a mixture of two compounds was found to exist with the same Fe: Mn ratio.<sup>210</sup> The two compounds are cubic spinels with the same crystallographic parameters; however, one compound is a defect spinel while the other is not. A similar work has been done by Delgado and co-workers.<sup>208</sup> In another study, Goldwasser *et al.* synthesized five perovskite oxides containing La, K, Fe and Mn<sup>209</sup> and observed that the activity of the solids in F–T synthesis is strongly dependent on the presence of Fe carbides. Mn was found to increase significantly the production of alkenes, and the combined presence of K and Mn resulted in a stable catalyst with a high yield of C<sub>2</sub>–C<sub>4</sub> alkenes.

More recently, Koizumi *et al.* observed that Mn has an additional beneficial effect in unsupported Fe-based F–T catalysts.<sup>211</sup> These authors studied the sulfur resistance of Mn–Fe catalysts and they observed superior catalyst stabilities, especially when the catalysts were pre-reduced in CO. This group also used IR spectroscopy in combination with CO as a probe molecule to compare Fe and Mn–Fe catalysts. It was found that the addition of Mn led to the appearance of several well-resolved bands upon CO adsorption. The appearance of the bands arising from bridged-bonded CO on Fe<sup>0</sup> indicated that the size of the Fe<sup>0</sup> particles were clearly larger than in the case of the unpromoted catalysts. They attributed the decreased reactivity towards H<sub>2</sub>S to the observed increase in Fe<sup>0</sup> particle size.

**4.1.2 Supported Fe–Mn Fischer–Tropsch Catalysts.** A much more limited number of studies have dealt with supported Mn-promoted Fe F–T catalysts. In this respect, it is worthwhile to mention the work of Xu *et al.*<sup>212</sup> These authors added MnO to a Fe/silicalite catalyst and observed an enhanced selectivity towards light olefins. Meanwhile the yields for methane as well as for CO<sub>2</sub> formation were almost unaffected by MnO addition. Moreover, the conversion of CO was also insensitive to the addition of the MnO promoter.

The results also indicated that the addition of MnO leads to an increased CO adsorption capacity. Das and co-workers also reported on the addition of Mn to silicalite supported Fe catalysts.<sup>205</sup> They observed that the addition of Mn reduces the particle size of the iron oxide precursor, leading to an increase in alkene selectivity. Another important study is by Abbot *et al.*<sup>213</sup> This group studied the addition of Mn to alumina-supported Fe catalysts and found that promotion led to an increase in the selectivity towards light olefins and a suppression of the selectivity towards methane. These effects were attributed to a change in the Fe dispersion (structural promotion) as well as to an electronic promotion.

**4.1.3 Mn-promoted Ru-based Fischer–Tropsch Catalysts.** To the best of our knowledge, the first claim on Mn-promoted Ru F–T catalysts was made in the patent literature by Kugler and co-workers.<sup>214</sup> Furthermore, it seems that only the group of Hussain have investigated these catalyst systems in great detail.<sup>215–227</sup> Hussain *et al.* observed that the addition of Mn to Ru/Al<sub>2</sub>O<sub>3</sub>, Ru/SiO<sub>2</sub> and Ru/TiO<sub>2</sub> catalysts produced new or improved active CO hydrogenation sites, which are responsible for the enhancement in the production of high molecular weight as well as unsaturated hydrocarbons. The authors discussed the addition of Mn in terms of an electronic and geometrical modification of the catalytically active Ru surface. In a continuation of their work, the same group used IR and CO as a probe molecule to characterize the metal surface of the supported Mn–Ru catalysts. The results indicated that Mn was present as a covering layer on the surface of the supported Ru nanoparticles. An increasing Mn loading led to a decreasing CO adsorption capacity, indicating that the excess of Mn masked the active Ru sites responsible for CO adsorption. No CO adsorption was found to occur on isolated Mn sites. In addition, it was found that the addition of Mn resulted in (1) the formation of a low frequency band in the IR spectrum and (2) a shift of the IR bands of Ru-adsorbed CO. Both observations were explained in terms of an electronic promotion effect, giving rise to different electronic properties of the surface Ru sites as well as changes in their local geometry. A necessary condition for promotion is that small Mn oxides decorate the surface of the supported Ru nanoparticles. Related to this decoration of the Ru surface, it is anticipated that the sites responsible for the production of CH<sub>4</sub> are blocked by the addition of Mn.

In order to gain additional information on the promotion effect of Mn, Hussain performed XPS, and static secondary ion mass spectrometry (SSIMS), to investigate the adsorption of adsorbed CO on the supported Mn–Ru F–T catalysts.<sup>223</sup> XPS revealed that the addition of CO causes a negative binding energy shift of the Ru peak on silica- and alumina-supported catalyst systems. This shift was higher on the corresponding Mn-promoted catalysts. This was attributed to the combined effect of Ru and Mn on the CO adsorption geometry. On titania-supported systems the unusual shift in Ru binding energy is the result of the formation of TiO<sub>x</sub> covering the surface due to the SMSI effect. The SSIMS data further supported the findings of the XPS study and RuCO<sup>+</sup>, RuO<sup>+</sup>, MnO<sup>+</sup> peaks were obtained. No evidence for CO adsorption



on Mn or MnO could be detected. All the experimental findings were consistent with the presence of linearly bonded CO on top of Ru nanoparticles supported on Al<sub>2</sub>O<sub>3</sub> and SiO<sub>2</sub>.

The SMSI effect in Mn-promoted Ru/TiO<sub>2</sub> catalysts was studied in more detail making use of the SSIMS technique, as well as with TEM, and selective chemisorption experiments.<sup>224</sup> The SSIMS technique revealed the presence of TiO<sub>x</sub> forming two new surface sites, TiO<sub>x</sub>-Ru and TiO-Mn. These species were found to be located at the immediate vicinity of the Ru nanoparticles. These new surface sites were considered to alter the electronic properties of the Ru metal surface and, as a consequence, the product selectivity.

A similar study was performed by the same group on a model catalyst system; *i.e.*, a Mn/Ru (0001) surface, prepared by sputtering Mn on a Ru (0001) surface at room temperature using a sputtered ion gun.<sup>222</sup> The techniques of choice were SSIMS, EELS and TPD. It was concluded that Mn reduces the coverage of CO adsorbed on the surface by physically blocking the adsorption sites. The adsorbed CO molecule is predominantly linearly bonded, whereas EELS indicated a possible existence of an electronic interaction between the deposited Mn and Ru. This was reflected by the change in the CO stretching frequency to lower wavenumbers once Mn was deposited on the Ru surface.

Tercioglu and Akyurtlu also studied the Mn promotion effect on Ru/Al<sub>2</sub>O<sub>3</sub> catalysts.<sup>228</sup> They observed that the three catalysts under study, 2.5 wt% Ru/Al<sub>2</sub>O<sub>3</sub>, 6.3 wt% Mn-2.5 wt% Ru/Al<sub>2</sub>O<sub>3</sub> and 6.3 wt% Mn-5 wt% Ru/Al<sub>2</sub>O<sub>3</sub>, showed different olefin selectivities. It was found that (1) the manganese-containing catalysts had higher selectivity for ethylene, which was three times higher than the corresponding unpromoted catalyst, and (2) the olefin-to-paraffin ratio was also affected by the presence of Mn and increased with increasing Mn content. The authors also noticed a similar influence of the Ru:Mn ratio on the formation of longer chain hydrocarbons. Finally, Shapovalova and Zakumbaeva studied Mn-promoted Ru/Al<sub>2</sub>O<sub>3</sub> catalysts with adsorption microcalorimetry, XPS and IR.<sup>229</sup> They concluded that Mn also acts as a structural promoter since it increases the dispersion of the Ru nanoparticles.

*4.1.4 Mn-promoted Co-based Fischer-Tropsch Catalysts. – 4.1.4.1 Unsupported Co-Mn Fischer-Tropsch Catalysts.* Van der Riet *et al.* were the first to report on the use of Mn as promoter in unsupported Co-based F-T catalysts.<sup>230</sup> They reported on a stable Co-containing CO hydrogenation catalyst with a high selectivity for C<sub>3</sub> hydrocarbons and suppressed CH<sub>4</sub> selectivity. This finding was rationalized in terms of competing hydrogenation and oligomerization reactions of the primary hydrocarbon products. In continuation of this work, Hutchings *et al.* reported in a detailed investigation on the mechanism of CO hydrogenation catalyzed by a Mn-Co catalyst.<sup>231</sup> The results of this study indicate that hydroformylation of a C<sub>2</sub> surface intermediate cannot account for the high yields of propene and the low yields of methane observed. Based on their findings, a reaction mechanism for carbon-carbon bond formation was proposed involving  $\alpha$ -hydroxylated metal-alkyl as an

important intermediate, the formation of which involves the coupling of a number of electrophilic and nucleophilic  $C_1$  surface intermediates. *In-situ* XRD studies of the same research group showed that the active catalysts contained bcc metallic Co supported on MnO.<sup>232</sup> This uncommon phase is metastable and readily transforms into the stable fcc structure after exposure to air and slight pressure at room temperature.

Based on this work and that of many other research groups<sup>233–239</sup> it can be stated that oxidized Mn–Co unsupported catalysts are composed of mixed cobalt manganese spinels of  $Co_2MnO_4$  and  $CoMn_2O_4$ , the ratio of which depends upon composition and pretreatment of the catalyst materials. Reduction of the catalysts in  $H_2$  results in a material that contains metallic cobalt, MnO and a certain amount of mixed spinels. An interesting study in line with the above description was reported by Liang *et al.*<sup>233</sup> These authors investigated in detail the influence of the preparation method of Co/Mn oxides and their corresponding Co/Mn ratios on the hydrogenation of CO. Nanometer spinel-type Co/Mn oxides with different Co/Mn ratios ( $Co_{3-x}Mn_xO_4$ ,  $0 < x < 1.4$ ), single phase composition and large specific surface area ( $> 70 \text{ m}^2/\text{g}$ ) were prepared by the sol-gel method. These materials were compared with those prepared by nitrate decomposition and solid-state reaction methods. CO hydrogenation tests indicated that the nanometer Co/Mn oxide catalysts had much higher selectivities for light olefins and possessed a lower catalytic activity and methane production capability than the corresponding coprecipitated catalysts with the same composition.

*In-situ* IR experiments on Co and Mn–Co F–T catalysts were performed by Jiang *et al.* to study in more detail the effect of the addition of Mn on the surface properties of the catalyst materials.<sup>237</sup> The authors used CO and  $CO + H_2$  as probe molecules under flowing conditions. It was found that metallic cobalt particles are formed on both Co and Mn–Co catalysts after reduction. This was manifested by the occurrence of the bands corresponding to CO adsorbed on  $Co^0$  sites. On the reduced Co sample, however, the molecularly adsorbed CO species were rather difficult to detect because of the rapid dissociation of CO on the fine active metallic cobalt particles formed. For the Mn–Co catalyst, however, distinct IR bands appeared and their intensities increased with increasing Mn loading. These bands were attributed to linearly, bridged, and multiply bridged-bonded CO. The authors considered that the sizes of the Co particles in the reduced Mn–Co catalyst were larger than those in the reduced Co catalyst, and that the stability of the Co particles could be remarkably enhanced with the incorporation of Mn promoter. This enhanced catalyst stability might be manifested by a decreased deactivation and an increased  $H_2S$  tolerance.

Keyser *et al.* studied Mn–Co F–T catalysts and found that, under industrial relevant conditions, the WGS activity of the catalysts increases with increasing Mn content, but decreases with increasing pressure.<sup>234,235</sup> A lower olefin yield was also observed at high pressures. It was stated that structural changes in the cobalt spinel occur over a long period of time and are responsible for the increased hydrogenation activity and increased WGS activity. Mn seems in this

respect not to be able to stabilize the cobalt spinel structure in order to retain the olefin activity. Finally, Riedel *et al.* also noticed the WGS activity of MnO and the addition of this compound to Co F–T catalysts led to the production of CO<sub>2</sub>.<sup>238</sup> In other words, Mn can be regarded as a water-gas shift promoter under F–T conditions.

*4.1.4.2 Supported Co–Mn Fischer–Tropsch Catalysts.* F–T synthesis of lower hydrocarbons on silicalite-1 supported Co and Co–Mn catalysts was reported by Das *et al.*<sup>110,119</sup> Co<sub>3</sub>O<sub>4</sub> was found to be the only phase present in Mn-free catalysts after calcination, while the addition of Mn favored the formation of a mixed spinel structure of the type (Co<sub>1–x</sub>Mn<sub>x</sub>)<sub>3</sub>O<sub>4</sub>. They considered that the addition of Mn decreased the reduction temperature of Co<sub>3</sub>O<sub>4</sub> and presumably its particle size. The catalysts showed good activity and selectivity for light hydrocarbons in the C<sub>2</sub>–C<sub>4</sub> range, particularly propene, and also showed very low WGS activity. Furthermore, the addition of Mn increased the CO conversion, while the selectivity towards alkenes slightly decreased.

Another interesting use of zeolites in F–T catalysis is the addition of pentasil zeolites, *e.g.* ZSM-5, to the unsupported Mn–Co F–T catalyst in order to shift the product distribution.<sup>109</sup> Two modes of operation were tested. The first was a single bed reactor with a mechanical mixture of the two components. The second mode of operation consisted of a dual bed approach with the Mn–Co and zeolite in separate reactors. This method of operation led to the formation of aromatic compounds, due to the transformation of olefinic and oxygen containing hydrocarbons. Additionally, high molecular weight hydrocarbons were cracked into lower alkanes. It was concluded that the dual bed arrangement with separate reactors was preferred since it allowed to adjust the optimum temperature for the F–T as well as the zeolite system and to regenerate the zeolite component independently.

Zhang *et al.* studied the Mn promotion in Co/Al<sub>2</sub>O<sub>3</sub> catalysts.<sup>116</sup> It was found that the addition of Mn improves the catalytic activity, as well as the C<sub>5+</sub> selectivity, while the formation of methane and C<sub>2–4</sub> hydrocarbons is significantly suppressed. They observed that Mn improved the dispersion of the active Co phase and also favored the formation of bridged-bonded CO as probed with IR. A small amount of Mn was also able to increase the H<sub>2</sub> uptake, although it was again decreased with an excess of Mn.

A very detailed characterization study on Mn-promoted Co/SiO<sub>2</sub> catalysts was carried out by the group of Klabunde.<sup>112,113</sup> They prepared their catalyst materials making use of the solvated metal atom dispersion (SMAD) technique. In this process metal atoms such as Co and Mn are solvated at low temperatures in toluene or other appropriate solvents. Upon warming the nucleation begins. The catalysts prepared were investigated with EXAFS and tested in the hydrogenation reaction of olefins. It was found that the reduced catalysts contained Mn in the oxidized state and Co in both the metallic and oxidized state. The presence of Mn might permit an appreciable increase in metallic Co. The EXAFS results also indicated that the most active Mn–Co/SiO<sub>2</sub> catalyst had the largest amount of metallic cobalt and it was argued that the more

oxophilic metal, Mn, would scavenge oxygen, allowing Co to remain in the metallic state. Chemisorption studies revealed that the addition of Mn increased the Co dispersion and it was proposed that Mn, in addition to aiding in the dispersion, also influenced the catalytic performances by an electronic effect. The authors also noticed that Mn was most probably bound to the support as a highly dispersed MnO phase, while Co was stabilized in a metallic form on the MnO.

The effects of Mn promoter on Co/TiO<sub>2</sub> catalysts were investigated by Voß *et al.*<sup>117</sup> They observed that the formation of CoTiO<sub>3</sub> was more strongly evident in the presence of Mn. XPS revealed that Mn was much more dispersed than Co in the catalyst system and no appreciable shifts in Co2p XPS binding energies were noticed when Mn was present in the catalyst. Mn was in the reduced catalysts present as MnO and it was assumed that MnO had no influence on the catalytic properties and served as an additional support.

Recently, Martinez *et al.* reported the use of mesoporous Co/SBA-15 catalysts promoted with Mn for the F–T synthesis.<sup>114</sup> They observed that Mn favored the formation of long-chain n-paraffins (C<sub>10+</sub>), while decreasing the selectivity towards methane. The Mn-promoted catalysts, however, turned out to be less active than the unpromoted ones.

In recent years our research group has been studying in more detail the Mn promotion in F–T Co/TiO<sub>2</sub> catalysts, using advanced characterization techniques, such as XAS, EXAFS, STEM-EELS and XPS.<sup>247–250</sup> We found that the preparation method largely influences the state and location of Mn promoter in Co/Mn/TiO<sub>2</sub> oxidized catalysts,<sup>249</sup> and it was shown that the incipient wetness impregnation method leads to the formation of small MnO<sub>2</sub> particles located on the TiO<sub>2</sub> surface, and also a highly dispersed MnO<sub>2</sub> phase. In contrast, the use of the homogeneous deposition precipitation method leads to the deposition of MnO<sub>2</sub> species preferentially on top of the Co<sub>3</sub>O<sub>4</sub> nanoparticles. This is evidenced by STEM-EELS, which revealed the elemental distribution of the Co/Mn/TiO<sub>2</sub> catalysts in chemical maps. In addition, EXAFS results at the Mn K-edge indicated the formation of mixed oxide compounds between Co and Mn; *i.e.*, the formation of Co<sub>3–x</sub>Mn<sub>x</sub>O<sub>4</sub> solid solutions occurs to some extent, causing an elongation of the Mn–O interatomic distances. In a related work,<sup>248</sup> we reported that Mn decreased the reducibility of the surface of the Co nanoparticles in Co/Mn/TiO<sub>2</sub> catalysts, resulting in catalysts with more unreduced cobalt phase. These findings were revealed by XAS results at the Co L<sub>2,3</sub> edges. It was reported that reduction of Co/TiO<sub>2</sub> and Co/Mn/TiO<sub>2</sub> catalysts, as well as bulk Co<sub>3</sub>O<sub>4</sub> material, at conditions of 2 mbar and 425°C, resulted in different amounts of Co<sup>0</sup> and CoO. The Co reducibility was strongly influenced by the TiO<sub>2</sub> support and the Mn oxides, given that bulk Co<sub>3</sub>O<sub>4</sub> was 100% reduced to Co<sup>0</sup>, whereas the TiO<sub>2</sub>-supported catalysts were only reduced to mixtures of CoO (60–75%) and Co<sup>0</sup>. This result was considered to be due to the SMSI effect occurring in these catalytic systems. The Mn-promoted catalyst was found to contain the least amount of Co<sup>0</sup>, indicating a decrease of the Co reducibility due to Mn. In other work using XPS,<sup>250</sup> we reported similar effects of the Mn promoter on the Co

reducibility. Both a Co/TiO<sub>2</sub> and Co/Mn/TiO<sub>2</sub> catalyst were reduced in H<sub>2</sub> at 350°C achieving high reduction degrees, although the Mn decreased the final amount of Co<sup>0</sup>. In addition, it was shown with quantitative XPS that the Mn oxides migrate upon reduction, from the top of the Co particles toward the TiO<sub>2</sub> surface. The Mn oxides were shown to segregate after reduction and to be enriched at the surface of TiO<sub>2</sub>. Nonetheless, some remaining MnO was also observed at the surface of the reduced Co nanoparticles. Based on EXAFS and STEM-EELS,<sup>249</sup> it was concluded that the Mn species might exist either in the form of MnO, which interacts with the Co nanoparticles, or in the form of Ti<sub>2</sub>MnO<sub>4</sub>, highly segregated at the outer layer of the TiO<sub>2</sub> surface. These titanate compounds are expected not to play a role in the F–T reaction, but to behave as spectator species. On the contrary, we interpreted that the MnO particles observed in close interaction with the Co<sup>0</sup> are able to induce an electronic promotion, resulting in the enhancement of the F–T selectivity. In this respect, we have reported in various papers significant changes in the F–T selectivity of Co/TiO<sub>2</sub> catalysts as a result of the addition of Mn.<sup>247–250</sup> The selectivity of the Mn-promoted catalysts has been shifted to higher C<sub>5+</sub> and lower methane production. In addition, the olefinic product was always increased in the case of the Co/Mn/TiO<sub>2</sub> catalysts. All these findings suggest a different probability of chain growth versus chain termination, influenced by the Mn oxides. Furthermore, the Mn was found to lower the hydrogenation rate occurring under F–T conditions causing an increase of the olefin product formed in the F–T synthesis.

Finally, it was observed by STEM-EELS that a Co/Mn/TiO<sub>2</sub> catalyst prepared by IWI clearly decreased the Co particle size after activation. Co<sup>0</sup> particles of 5–10 nm were covered by MnO after reduction, and this was manifested in the F–T reaction as a decrease in activity. Hence, it was concluded that even when Mn is not mixed with the Co<sub>3</sub>O<sub>4</sub> in the calcined catalyst, upon reduction it may undergo changes, which lead to a covering and blocking of the small Co particles by the MnO phase.

*4.1.5 General Observations Based on the Literature Survey.* From the above discussions it is evident that Mn promotion has been explored in more detail for unsupported than for supported F–T catalysts. Regardless of the type of support and the type of active F–T metal, similar trends are found regarding the promotion effect of Mn. The following conclusions can be drawn from this literature survey:

(1) Mn, when decorating as an oxide layer on top of the surface of the active metal, is clearly able to induce an electronic effect. This electronic promotion is evident from the effect on the catalyst selectivity, as well as on the CO IR adsorption properties (frequency shifts in metal-adsorbed CO). Moreover, XPS binding energy shifts have been observed, particularly for Ru-based F–T catalysts. Consequently, Mn–Co F–T catalysts possess decreasing hydrogenation properties compared to Co F–T catalysts, causing a shift in the product distribution towards more olefinic, and increasing the C<sub>5+</sub> production.

(2) Besides the electronic promotion effect, Mn may also induce structural and synergistic promotion effects and it has been occasionally reported to increase the metal dispersion and to improve the resistance of the catalyst material against  $\text{H}_2\text{S}$  and re-oxidation during operation. Moreover, Mn possesses WGS behavior and therefore can be regarded as a WGS promoter. One could therefore state that Mn-promotion makes supported Co nanoparticles more “Fe-like”.

(3) In order to achieve all these promotion effects, the preparation method clearly plays a role and it may be of no wonder that many studies have focused on the formation of a  $\text{M}_x\text{Mn}_y\text{O}_z$  (with M = active F–T metal; e.g., for Co,  $\text{Mn}_x\text{Co}_{3-x}\text{O}_4$ ) phase. This spinel oxide is broken up during reduction to make  $\text{MnO}_x$  and a metallic surface. Due to the pre-existence of this Mn–M interaction, electronic promotion is much more easily achieved after reduction as well. It is worthwhile to mention that  $\text{Mn}_x\text{Co}_{3-x}\text{O}_4$  compounds are well studied in the literature, because they have important electrocatalytical properties. More specifically, spinel-type manganese oxides are widely used as precursors in the preparation of  $\lambda\text{-MnO}_2$  ( $[\square]\text{A}[\text{Mn}_2]\text{BO}_4$ ), an oxide of technical interest due to its application as a cathode material for rechargeable cells.<sup>240–246</sup>

## 5 Concluding Remarks and Outlook

Fischer–Tropsch synthesis making use of cobalt-based catalysts is a hotly pursued scientific topic in the catalysis community since it offers an interesting and economically viable route for the conversion of e.g. natural gas to sulphur-free diesel fuels. As a result, major oil companies have recently announced to implement this technology and major investments are under way to build large Fischer–Tropsch plants based on cobalt-based catalysts in e.g. Qatar. Promoters have shown to be crucial to alter the catalytic properties of these catalyst systems in a positive way. For this reason, almost every chemical element of the periodic table has been evaluated in the open literature for its potential beneficial effects on the activity, selectivity and stability of supported cobalt nanoparticles.

The addition of promoter elements to cobalt-based Fischer–Tropsch catalysts can affect (1) directly the formation and stability of the active cobalt phase (*structural promotion*) by altering the cobalt-support interfacial chemistry, (2) directly affect the elementary steps involved in the turnover of the cobalt active site by altering the electronic properties of the cobalt nanoparticles (*electronic promotion*) and (3) indirectly the behaviour of the active cobalt phase, by changing the local reaction environment of the active site as a result of chemical reactions performed by the promoter element itself (*synergistic promotion*).

Despite major research efforts, not so much fundamental insights exist in the origin and the exact mode of operation of these promotion effects. Furthermore, the same promoter can exhibit several effects on the catalyst performances. In addition, there are some contradictions in the literature on the proposed effects of specific promoter elements. Several reasons can be put forward to explain these general observations:

(1) Promoted cobalt-based F–T catalysts are from material scientist perspective very complex systems. As a consequence, most characterization techniques, including surface as well as bulk spectroscopies, are not suitable for discriminating between the multiple cobalt and promoter species present at the surface of the support oxide. The existence of spectator species, as a result of the formation of solid compounds between the cobalt oxide and support oxide (*e.g.*  $\text{CoTiO}_3$ ) and between the promoter element and the support oxide (*e.g.*  $\text{Ti}_2\text{MnO}_4$ ), may further complicate this task. As a result, only detailed physicochemical insight can be obtained by making use of a combination of advanced characterization techniques. Since each technique has its own sensitivity towards the different active and spectator species present at the catalyst surface, a more complete picture will only emerge by combining the information gathered by the different spectroscopic techniques employed.

(2) Promoter elements only exhibit their beneficial effect in a limited concentration range as the addition of the promoters in a too high amount may lead to a complete decoration of the active cobalt surface, and as a consequence, result in a decrease of the catalyst activity. In addition, the preparation method is crucial in achieving the envisaged promotion effect. Both arguments may be responsible for the conflicting views in the literature on the different promotion effects of a specific element added to the catalyst material. On the other hand, all this indicates that catalyst preparation tools should be improved to add promoter elements in a precise and controlled manner to the catalyst material. It is, however, important to recall that such synthesis tools should be at a later stage still attractive to the large-scale industrial production of cobalt-based Fischer–Tropsch catalysts.

(3) It is far from easy to distinguish structural, electronic and synergistic promotion effects. Structural promotion is, in this respect, the most easily to observe. Most synergistic effects are also widely discussed in the literature in enhancing the catalytic performance of supported cobalt nanoparticles. Instead, promotion as a result of electronic effects are much more difficult to detect. The main reason is that one has to discriminate between the number of surface cobalt sites and the intrinsic activity of a surface cobalt site (turnover frequency). This is especially difficult in view of the complexity of the catalyst material. It also requires spectroscopic tools, which are able to detect changes in the electronic structure of the supported cobalt nanoparticles.

(4) The characterization tools to investigate cobalt-based Fischer–Tropsch catalysts are mostly used to study the catalyst materials under conditions far from industrially relevant reaction conditions; *i.e.*, in the presence of CO and  $\text{H}_2$ , as well as of the reaction products, including  $\text{H}_2\text{O}$ ; at reaction temperatures and at high pressures. Since catalytic solids are dynamic materials undergoing major changes under reaction conditions it can be anticipated that the currently obtained information on the active site is at least incomplete. This holds also for the active state and location of the promoter element under reaction conditions. For example, an electronic effect on the cobalt active phase induced by a promoter element can maybe exist only at high pressures and will remain – due to the lack of the appropriate instrumentation – unnoticed to the catalyst

scientist. Therefore, major efforts should be directed to the development of advanced *in-situ* spectroscopy-microscopy techniques to study promoted Co-based Fischer–Tropsch catalysts in action.

Summarizing, there are still many scientific challenges and major opportunities for the catalysis community in the field of cobalt-based Fischer–Tropsch synthesis to design improved or totally new catalyst systems. However, such improvements require a profound knowledge of the promoted catalyst material. In this respect, detailed physicochemical insights in the cobalt-support, cobalt-promoter and support-support interfacial chemistry are of paramount importance. Advanced synthesis methods and characterization tools giving structural and electronic information of both the cobalt and the support element under reaction conditions should be developed to achieve this goal.

## Acknowledgments

The authors gratefully acknowledge financial support from Shell Global Solutions, leading to the results reported in this review paper. B.M.W. also acknowledges financial support from NWO (Van der Leeuw and VICI grants) for his research on *in-situ* catalyst characterization. The work also benefited from fruitful discussions with H. Oosterbeek, H. Kuipers and C. Mesters of Shell Global Solutions. Finally, the authors thank E. Kuipers (Engelhard), A. Buchanan (Sasol) and A. Rautenbach (Sasol) for kindly providing us with Figures 1 and 2. Both pictures originate from Sasol Limited<sup>®</sup>.

## References

1. A historical account on Fischer–Tropsch synthesis can be found on the web: [http://www.Fischer–Tropsch.org](http://www.Fischer-Tropsch.org).
2. F. Fischer and H. Tropsch, *Brennstoff-Chemie*, 1926, 97.
3. E.J. Hoffman, *Coal Conversion*, The Energon Company, Laramie, Wyoming, 1970, p. 223.
4. J. Patzlaff, Y. Lieu, C. Graffmann and J. Gaube, *Appl. Catal. A: General*, 1999, **186**, 109.
5. J.H. Gregor, *Catal. Lett.*, 1990, **7**, 317.
6. H. Schulz, *Appl. Catal. A: General*, 1999, **186**, 3.
7. D.J. Duvenhage and T. Shingles, *Catal. Today*, 2002, **71**, 227.
8. S.T. Rie and R. Kirshna, *Appl. Catal. A: General*, 1999, **186**, 55.
9. B. Jager and R. Espinoza, *Catal. Today*, 1995, **23**, 17.
10. P.J. Van Berge, S. Barradas, J. Van de Loodsdrecht and J.L. Visage, *Petrochemie*, 2001, **138**.
11. T.H. Fleisch, R.A. Sills and M.D. Briscoe, *J. Nat. Gas. Chem.*, 2002, **11**, 1.
12. P.J. Van Berge, S. Barradas, J. Van de Loodsdrecht and J.L. Visage, *Erdoel, Erdgas, Kohle*, 2001, **117**, 138.
13. J.G. Goodwin, *Proc. of ACS Symp, Methane Upgrading*, Atlanta, GA, USA, 1991, p. 156.
14. E. Iglesia, *Appl. Catal. A: General*, 1997, **161**, 59.
15. E. Iglesia, S.C. Reyes, R.J. Madon and S.L. Soled, *Adv. Catal.*, 1993, **39**, 221.
16. M.E. Dry, in *Catalysis Science and Technology*, eds. J.R. Anderson and M. Boudart Vol. 1, Springer, Berlin, 1981, p. 159.



17. M.E. Dry, *J. Chem. Technol. Biotechnol.*, 2001, **77**, 43.
18. M.E. Dry, *Appl. Catal. A: General*, 1996, **138**, 319.
19. M.E. Dry, *Catal. Today*, 2002, **71**, 227.
20. M.E. Dry, *Appl. Catal. A: General*, 2004, **276**, 1.
21. For more details we refer to the following website: <http://www.sasol.com>.
22. Shell press release on March 9 2004 (<http://www.shell.com>).
23. ExxonMobil press release on July 14 2004 (<http://www.exxonmobil.com>).
24. J. Jacometti, A. Ekvall, Shell in the Middle East, issue 17, April 2002, 1–3.
25. G. Coupe, Step on the gas, in *The Engineer*, August 6, 2004.
26. F. Thackeray, *Fischer–Tropsch GTL Approaches Treshold*, in *World Petroleum Congress*, 2003, pp. 150–151.
27. A.H. Tullo, Catalyzing GTL, *Chem. Eng. News*, 2003, **81**, 18.
28. The picture shows the Sasol Slurry Phase Distillate (SPD™) process plant, which converts at low temperatures synthesis gas to paraffins and specialty waxes. We express our gratitude to A. Buchanan and A. Rautenbach, both from Sasol, for kindly providing us with these figures.
29. V. Ponec, in *Handbook of Heterogeneous Catalysis*, eds. G. Ertl, H. Knozinger and J. Weitkamp, Wiley-VCH, Weinheim, 1997, p. 1876.
30. B. Cornils, W.A. Herrmann, R. Schlögl and C.H. Wong, *Catalysis from A to Z, A concise encyclopedia*, Wiley-VCH, Weinheim, 2000.
31. J. Hagen, *Industrial Catalysis, A practical approach*, Wiley-VCH, Weinheim, 1999, p. 174.
32. J.C. Geerling, J.H. Wilson and G.J. Kramer, *Appl. Catal. A: General*, 1999, **186**, 27.
33. A.A. Adesina, *Appl. Catal. A: General*, 1996, **138**, 345.
34. M.E. Dry, *Appl. Catal. A: General*, 1999, **189**, 185.
35. B. Jager, *Stud. Surf. Sci. Catal.*, 1997, **107**, 207.
36. B. Davis, *Fuel Proc. Techn.*, 2001, **71**, 157.
37. A.C. Vosloo, *Fuel Proc. Techn.*, 2001, **71**, 149.
38. M.J. Overett, R.O. Hill and J.R. Moss, *Coord. Chem. Rev.*, 2000, **206–207**, 581.
39. I. Wender, *Fuel Processing Technology*, 1996, **48**, 228.
40. R.L. Espinoza, A.P. Steynberg, B. Jager and A.C. Vosloo, *Appl. Catal. A: General*, 1999, **186**, 13.
41. R.B. Anderson, *The Fischer Tropsch Synthesis*, Academic Press, New York, 1984.
42. A.T. Bell, H. Heinemann and W.G. McKee, *Appl. Catal.*, 1982, **2**, 219.
43. E. Iglesia, S.L. Soled and R.A. Fiato, *J. Catal.*, 1993, **143**, 345.
44. M. Hoang, A.E. Hughes and T.W. Turney, *Appl. Surf. Sci.*, 1993, **72**, 55.
45. L.A. Bruce, M. Hoang, A.E. Hughes and T.W. Turney, *Appl. Catal. A: General*, 1993, **100**, 51.
46. E. Iglesia, S.L. Soled, R.A. Fiato and G.H. Via, *Stud. Surf. Sci. Catal.*, 1994, **81**, 433.
47. J. Vaarl, J. Lahtinen and P. Hautajarvi, *Surf. Sci.*, 1996, **346**, 11.
48. C.L. Bianchi, R. Carli, S. Merlotti and V. Ragaini, *Catal. Lett.*, 1996, **41**, 79.
49. A. Kogelbauer, J.G. Goodwin and R. Oukaci, *J. Catal.*, 1996, **160**, 125.
50. G.D. Zakumbayeva, L.B. Shapovalova, I.G. Yefremenko and A.V. Gabdrakipov, *Petroleum Chem.*, 1996, **36**, 428.
51. A.R. Belambe, R. Oukaci and J.G. Goodwin, *J. Catal.*, 1997, **166**, 8.
52. J.G. Price, D. Glasser, D. Hildebrandt and N.J. Coville, *Stud. Surf. Sci. Catal.*, 1997, **107**, 243.
53. E. Iglesia, *Stud. Surf. Sci. Catal.*, 1997, **107**, 153.

54. M. Niemela, M. Reinikainen and J. Kiviaho, *Stud. Surf. Sci. Catal.*, 1998, **118**, 229.
55. C.L. Bianchi, S. Vitali and V. Ragaini, *Stud. Surf. Sci. Catal.*, 1998, **119**, 167.
56. M. Reinikainen, M.K. Niemela, N. Kakuta and S. Suhonen, *Appl. Catal. A: General*, 1998, **174**, 61.
57. L. Guzzi, G. Stefler, Z. Koppany, V. Komppa and M. Reinikainen, *Stud. Surf. Sci. Catal.*, 1999, **121**, 209.
58. P.M. Maitlis, R. Quyoum, H.C. Long and M.L. Turner, *Appl. Catal. A: General*, 1999, **186**, 363.
59. Y. Borodko and G.A. Somorjai, *Appl. Catal. A: General*, 1999, **186**, 355.
60. M. Kraum and M. Baerns, *Appl. Catal. A: General*, 1999, **186**, 189.
61. Y.L. Zhang, D.G. Wei, S. Hammache and J.G. Goodwin, *J. Catal.*, 1999, **188**, 281.
62. L. Huang and Y. Xu, *Catal. Lett.*, 2000, **69**, 145.
63. J.L. Li, L.G. Xu, R. Keogh and B. Davis, *Catal. Lett.*, 2000, **70**, 127.
64. L. Huang and Y.D. Xu, *Appl. Catal. A: General*, 2001, **205**, 183.
65. H.A.J. van Dijk, J.H.B. Hoebink and J.C. Schouten, *Chem. Eng. Sci.*, 2001, **56**, 1211.
66. G. Jacobs, Y. Zhang, T.K. Das, J. Li, P.M. Patterson and B.H. Davis, *Stud. Surf. Sci. Catal.*, 2001, **139**, 415.
67. B. Jongsomjit, J. Panpranot and J.G. Goodwin, *J. Catal.*, 2001, **204**, 98.
68. S. Hammache, J.G. Goodwin and R. Oukaci, *Catal. Today*, 2002, **71**, 361.
69. S. Sun, K. Fujimoto, Y. Yoneyama and N. Tsubaki, *Fuel*, 2002, **81**, 1583.
70. J. Panpranot, J.G. Goodwin and A. Sayari, *J. Catal.*, 2002, **211**, 530.
71. M.L. Turner, N. Marsih, B.E. Mann, R. Quyoum, H.C. Long and P.M. Maitlis, *J. Am. Chem. Soc.*, 2002, **124**, 10456.
72. J. Panpranot, J.G. Goodwin and A. Sayari, *Catal. Today*, 2002, **77**, 269.
73. J. Panpranot, J. G. Goodwin and A. Sayari, *J. Catal.*, 2003, **213**, 78.
74. D. Bazin, I. Kovacs, J. Lynch and L. Guzzi, *Appl. Catal. A: General*, 2003, **242**, 179.
75. L.B. Shapovalova, G.D. Zakumbaeva and A.V. Gabdrakipov, *Petroleum Chem.*, 2003, **43**, 170.
76. M. Shinoda, Y. Zhang, Y. Shiki, Y. Yoneyama, K. Hasegawa and N. Tsubaki, *Catal. Comm.*, 2003, **4**, 423.
77. M. Johns, P. Collier, M.S. Spencer, T. Alderson and G.J. Hutchings, *Catal. Lett.*, 2003, **90**, 187.
78. H.A.J. van Dijk, J.H.B.J. Hoebink and J.C. Schouten, *Top. Catal.*, 2003, **26**, 111.
79. H.A.J. van Dijk, J.H.B.J. Hoebink and J.C. Schouten, *Top. Catal.*, 2003, **26**, 163.
80. F.M.T. Mendes, F.B. Noronha, C.D.D. Sluza, M.A.P. da Silva, A.B. Gaspar and M. Schmal, *Stud. Surf. Sci. Catal.*, 2004, **147**, 361.
81. S.A. Hosseini, A. Taeb, F. Feyzi and F. Yaripour, *Catal. Comm.*, 2004, **5**, 137.
82. L.B. Shapovalova, G.D. Zakumbaeva and A.A. Zhurtbaeva, *Stud. Surf. Sci. Catal.*, 2004, **147**, 373.
83. G.D. Zakumbaeva and L.B. Shapovalova, *Petr. Chem.*, 2004, **44**, 334.
84. M. Cerro-Alarcon, A. Maroto-Valiente, I. Rodriguez-Ramos, A. Guerrero-Ruiz, D. Schanke, A.M. Hilmen, E. Bergene, K. Kinnari, E. Rytter, E. Adnanes and A. Holmen, *Catal. Lett.*, 1995, **34**, 269.
85. L.E.S. Rygh, I. Gausemel, O.H. Ellestad, P. Klæboe, C.J. Nielsen and E. Rytter, *J. Mol. Struct.*, 1995, **349**, 325.
86. A.M. Hilmen, D. Schanke and A. Holmen, *Catal. Lett.*, 1996, **38**, 143.
87. A.M. Hilmen, D. Schanke and A. Holmen, *Stud. Surf. Sci. Catal.*, 1997, **107**, 237.

88. A.M. Hilmen, D. Schanke, K.F. Hanssen and A. Holmen, *Appl. Catal. A: General*, 1999, **186**, 169.
89. L.E.S. Rygh and C.J. Nielsen, *J. Catal.*, 2000, **194**, 401.
90. A.M. Hilmen, E. Bergene, O.A. Lindvag, D. Schanke, S. Eri and A. Holmen, *Catal. Today*, 2001, **69**, 227.
91. M. Ronning, D.G. Nicholson and A. Holmen, *Catal. Lett.*, 2001, **72**, 141.
92. L. Guzzi, G. Stefler, Z. Koppány and L. Borko, *React. Kin. Catal. Lett.*, 2001, **74**, 259.
93. L. Guzzi, L. Takacs, G. Stefler, Z. Koppány and L. Borko, *Catal. Today*, 2002, **77**, 237.
94. D. Bazin, L. Borko, Z. Koppány, I. Kovacs, G. Stefler, L.I. Sajo, Z. Schay and L. Guzzi, *Catal. Lett.*, 2002, **84**, 169.
95. L. Guzzi, G. Stefler, L. Borko, Z. Koppány, F. Mizukami, M. Toba and S. Niwa, *Appl. Catal. A: General*, 2003, **246**, 79.
96. G. Jacobs, J.A. Chaney, P.M. Patterson, T.K. Das and B.H. Davis, *Appl. Catal. A: General*, 2004, **264**, 203.
97. C.J. Bertole, C.A. Mims and G. Kiss, *J. Catal.*, 2004, **221**, 191.
98. C. Aaserud, A.M. Hilmen, E. Bergene, S. Eric, D. Schanke and A. Holmen, *Catal. Lett.*, 2004, **94**, 171.
99. Z. Zsoldos, T. Hoffer and L. Guzzi, *J. Phys. Chem.*, 1991, **95**, 798.
100. L. Guzzi, T. Hoffer, Z. Zsoldos, S. Zyade, G. Maire and F. Garin, *J. Phys. Chem.*, 1991, **95**, 802.
101. G.M. Lu, T. Hoffer and L. Guzzi, *Catal. Lett.*, 1992, **14**, 207.
102. Z. Zsoldos and L. Guzzi, *J. Phys. Chem.*, 1992, **96**, 9393.
103. D. Schanke, S. Vada, E.A. Blekkan, A.M. Hilmen, A. Hoff and A. Holmen, *J. Catal.*, 1995, **156**, 85.
104. S. Tang, J. Lin and K.L. Tan, *Surf. Int. Anal.*, 1999, **28**, 155.
105. G.W. Huber, C.H. Bartholomew, T.L. Conrad, K.W. Woolley and C.G. Guymon, *Am. Chem. Soc. Abstracts*, 2000, **219**, 261.
106. J. Li, X. Zhang, Y. Zhang, G. Jacobs, T. Das and H. Davis, *Appl. Catal. A: General*, 2002, **228**, 203.
107. G. Jacobs, T.K. Das, P.M. Patterson, J. Li, L. Sanchez and B.H. Davis, *Appl. Catal. A: General*, 2003, **247**, 335.
108. G. Jacobs, J.A. Chaney, P.M. Patterson, T.K. Das, J.C. Maillot and B.H. Davis, *J. Synchrot. Rad.*, 2004, **11**, 414.
109. D.J. Koh, J.S. Chung and Y.G. Kim, *Ind. Eng. Chem. Res.*, 1995, **34**, 1969.
110. D. Das, G. Ravichandran and D.K. Chakrabarty, *Catal. Today*, 1997, **36**, 285.
111. G. Baurle, K. Guse, M. Lohrengel and H. Papp, *Stud. Surf. Sci. Catal.*, 1993, **75**, 2789.
112. B.J. Tan, K.J. Klabunde, T. Tanaka, H. Kanai and S. Yoshida, *J. Am. Chem. Soc.*, 1998, **110**, 5951.
113. K.J. Klabunde and Y. Imizu, *J. Am. Chem. Soc.*, 1984, **106**, 2721.
114. A. Martinez, C. Lopez, F. Marquez and I. Diaz, *J. Catal.*, 2003, **220**, 486.
115. H.Y. Gao, J.G. Chen, H.W. Xiang, J.L. Yang, Y.W. Li and Y.H. Sun, *Chin. J. Catal.*, 2001, **22**, 133.
116. J.L. Zhang, J. Ren, J.G. Chen and Y.H. Sun, *Acta Physico-Chimica Sin.*, 2002, **18**, 260.
117. M. Voß, D. Borgmann and G. Wedler, *J. Catal.*, 2002, **212**, 10.
118. C.H. Bartholomew and R.C. Reuel, *Ind. Eng. Chem. Prod. Res. Dev.*, 1985, **24**, 56.

119. D. Das, G. Ravichandran and D.K. Chakrabarty, *Appl. Catal. A: General*, 1995, **131**, 335.
120. J.L. Li and N.J. Coville, *Appl. Catal. A: General*, 1999, **181**, 201.
121. J.L. Li and N.J. Coville, *Appl. Catal. A: General*, 2001, **208**, 177.
122. N.J. Coville and J. Li, *Catal. Today*, 2002, **71**, 403.
123. J.L. Li and N.J. Coville, *South African J. Chem.*, 2003, **56**, 1.
124. J.L. Li and N.J. Coville, *Am. Chem. Soc. Abstracts*, 2003, **226**.
125. S. All, B. Chen and J.G. Goodwin, *J. Catal.*, 1995, **157**, 35.
126. R. Oukaci, J.G. Goodwin, G. Marcelin and A. Singleton, *Am. Chem. Soc. Abstracts*, 1995, **209**.
127. G.R. Moradi, M.M. Basir, A. Taeb and A. Kiennemann, *Catal. Comm.*, 2003, **4**, 27.
128. B. Jongsomjit, J. Panpranot and J.G. Goodwin, *J. Catal.*, 2003, **215**, 66.
129. W. Zhou, J.G. Chen and Y.H. Sun, *Chin. J. Catal.*, 2004, **25**, 467.
130. S. Vada, A.M. Kazi, F.K. Beduaddo, B. Chen and J.G. Goodwin, *Stud. Surf. Sci. Catal.*, 1994, **81**, 443.
131. S. Vada, B. Chen and J.G. Goodwin, *J. Catal.*, 1995, **153**, 224.
132. G.J. Haddad, B. Chen and J.G. Goodwin, *J. Catal.*, 1996, **161**, 274.
133. G.J. Haddad, B. Chen and J.G. Goodwin, *J. Catal.*, 1996, **160**, 43.
134. J. Vaari, J. Lahtinen, A. Talo and P. Hautojarvi, *Surf. Sci.*, 1991, **251**, 1096.
135. I. Puskas, T.H. Fleisch, J.B. Hall, B.L. Meyers and R.T. Roginski, *Stud. Surf. Sci. Catal.*, 1993, **75**, 2813.
136. M.K. Niemela and A.O.I. Krause, *Catal. Lett.*, 1995, **34**, 75.
137. A.F.Y. Alshammary, I.T. Caga, A.Y. Tata and J.M. Winterbotton, *Eur. J. Sol. State Inorg. Chem.*, 1991, **28**, 453.
138. X.P. Dai, C.C. Yu and S.K. Shen, *Chin. J. Catal.*, 2001, **22**, 104.
139. H.B. Shi, Q. Li, X.P. Dai, C.C. Yu and S.K. Shen, *Stud. Surf. Sci. Catal.*, 2004, **147**, 313.
140. E.A. Blekkan, A. Holmen and S. Vada, *Act. Chem. Scand.*, 1993, **47**, 275.
141. G.P. Huffman, H. Shan, J.M. Zhao, F.E. Huggins, T.E. Hoost, S. Halvorsen and J.G. Goodwin, *J. Catal.*, 1995, **151**, 17.
142. S.J. Jenkins and D.A. King, *J. Am. Chem. Soc.*, 2000, **122**, 10610.
143. G.W. Huber, S.J.M. Butala, M.L. Lee and C.H. Bartholomev, *Catal. Lett.*, 2001, **74**, 45.
144. H.K. Woo, R. Srinivasan, L. Rice, R.J. Deangelis and P.J. Reucroft, *J. Mol. Catal.*, 1990, **59**, 83.
145. J.E. Baker, R. Burch, S.J. Hibble and P.K. Loader, *Appl. Catal.*, 1990, **65**, 281.
146. A.L. Lapidus, A.Y. Krylova, M.P. Kapur, E.V. Leongardt, A.B. Fasman and S.D. Mikhailenko, *Bull. Russ. Acad. Sci.-Div. Chem. Sci.*, 1992, **41**, 45.
147. S.E. Colley, M.J. Betts, R.G. Copperthwaite, G.J. Hutchings and N.J. Coville, *J. Catal.*, 1992, **134**, 186.
148. A.F.Y. Alshammary, I.T. Caga, A.Y. Tata, J.M. Winterbottom and I.R. Harris, *J. Chem. Tech. Biotech.*, 1992, **55**, 375.
149. I.R. Harris, I.T. Caga, A.Y. Tata and J.M. Winterbottom, *Stud. Surf. Sci. Catal.*, 1993, **75**, 2801.
150. M.P. Kapoor, A.L. Lapidus and A.Y. Krylova, *Stud. Surf. Sci. Catal.*, 1993, **75**, 2741.
151. A.G. Ruiz, A.S. Escribano and I.R. Ramos, *Appl. Catal. A: General*, 1994, **120**, 71.
152. S. Bessell, *Stud. Surf. Sci. Catal.*, 1994, **81**, 479.
153. S. Vada, A. Of, E. Adnanes, D. Schanke and A. Holmen, *Top. Catal.*, 1995, **2**, 155.

154. J. Barrault and N. Biwole, *Bull. Soc. Chim. Belg.*, 1995, **104**, 149.
155. M. Niemela and M. Reinikainen, *Stud. Surf. Sci. Catal.*, 1998, **119**, 161.
156. D.O. Uner, *Ind. Eng. Chem. Res.*, 1998, **37**, 2239.
157. K. Okabe, X.H. Li, T. Matsuzaki, M. Toba, H. Arakawa and K. Fujimoto, *J. Jap. Petrol. Inst.*, 1999, **42**, 377.
158. E. Kikuchi, R. Sorita, H. Takahashi and T. Matsuda, *Appl. Catal. A: General*, 1999, **186**, 121.
159. A. Frydman, D.G. Castner, C.T. Campbell and M. Schmal, *J. Catal.*, 1999, **188**, 1.
160. S. Sun, N. Tsubaki and K. Fujimoto, *Chem. Lett.*, 2000, **2**, 176.
161. J.L. Li, L.G. Xu, R.A. Keogh and B.H. Davis, *Am. Chem. Soc. Abstracts*, 2000, **219**.
162. N. Tsubaki, S.L. Sun and K. Fujimoto, *J. Catal.*, 2001, **199**, 236.
163. K. Okabe, X.H. Li, T. Matsuzaki, H. Arakawa and K. Fukimoto, *J. Sol-Gel Sci. Tech.*, 2000, **19**, 519.
164. C.L. Bianchi, *Catal. Lett.*, 2001, **76**, 155.
165. D.G. Wei, J.G. Goodwin, R. Oukaci and A.H. Singleton, *Appl. Catal. A: General*, 2001, **210**, 137.
166. G. Jacobs, T.K. Das, Y.Q. Zhang, J.L. Li, G. Racoillet and B.H. Davis, *Appl. Catal. A: General*, 2002, **233**, 263.
167. G. Jacobs, P.M. Patterson, Y.Q. Zhang, T. Das, J.L. Li and B.H. Davis, *Appl. Catal. A: General*, 2002, **233**, 215.
168. J.L. Li, G. Jacobs, Y.Q. Zhang, T. Das and B.H. Davis, *Appl. Catal. A: General*, 2002, **223**, 195.
169. R.V. Belosludov, S. Skahara, K. Yajima, S. Takami, M. Kubo and A. Miyamoto, *Appl. Surf. Sci.*, 2002, **189**, 245.
170. T. Riedel and G. Schaub, *Top.Catal.*, 2003, **26**, 145.
171. A. Martinez, C. Lopez, F. Marquez and I. Diaz, *J. Catal.*, 2003, **220**, 486.
172. M. Wei, K. Okabe and H. Arakawa, *J. Jap. Petrol. Inst.*, 2003, **46**, 339.
173. W.S. Yang, D.H. Yin, J. Chang, H.W. Xiang, Y.Y. Xu and Y.W. Li, *Acta Chim. Sinica.*, 2003, **61**, 681.
174. F.M.T. Mendes, F.B. Noronha, C.D.D. Souza, M.A.P. da Silva, A.B. Gaspar and M. Schmal, *Stud. Surf. Sci. Catal.*, 2004, **147**, 361.
175. N. Koizumi, K. Murai, T. Ozaki and M. Yamada, *Catal. Today*, 2004, **89**, 465.
176. K. Nagaoka, K. Takanabe and K. Aika, *Appl. Catal. A: General*, 2004, **268**, 151.
177. D. Bazin and L. Guzzi, *Stud. Surf. Sci. Catal.*, 2004, **147**, 343.
178. G.L. Bezemer, A. van Laak, A.J. van Dillen and K.P. de Jong, *Stud. Surf. Sci. Catal.*, 2004, **147**, 259.
179. G.L. Bezemer, U. Falke, A.J. van Dillen and K.P. de Jong, *Chem. Commun.*, 2005, **731**.
180. P. Concepcion, C. Lopez, A. Martinez and V.F. Puentes, *J. Catal.*, 2004, **228**, 321.
181. A.Y. Khodakov, A. Griboval-Constant, R. Bechara and F. Villain, *J. Phys. Chem. B*, 2001, **105**, 9805.
182. A. Khodakov, A. Griboval-Constant, R. Bechara and V.L. Zholobenko, *J. Catal.*, 2002, **206**, 230.
183. D. Yin, W. Li, W. Yang, H. Xiang, Y. Sun, B. Zhong and S. Peng, *Microporous Mesoporous Mater.*, 2001, **47**, 15.
184. S. Suvato and T.A. Pakkanen, *J. Mol. Catal. A: Chemical*, 2000, **164**, 273.
185. J. Panpranot, J.G. Goodwing Jr. and A. Sayari, *Catal. Today*, 2002, **77**, 269.
186. A.Y. Khodakov, R. Bechara and A. Griboval-Constant, *Appl. Catal. A: General*, 2003, **254**, 273.

187. A. Martinez, C. Lopez, F. Marquez and I. Diaz, *J. Catal.*, 2003, **220**, 486.
188. D.J. Koh, J.S. Chung and Y.G. Kim, *Ind. Eng. Chem. Res.*, 1995, **34**, 1969.
189. Y. Ohtsuka, T. Arai, S. Takasaki and N. Tsubouchi, *Energy and Fuels*, 2003, **17**, 804.
190. A.M. Saib, M. Claeys and E. van Steen, *Catal. Today*, 2002, **71**, 395.
191. Z. Paal and G.A. Somorjai, in *Handbook of Heterogeneous Catalysis*, eds. G.Ertl, H.Knozinger and J. Weitkamp, Wiley-VCH, Weinheim, 1997, p. 1084.
192. *Preparation of Solid Catalysts*, eds. G. Ertl, H. Knozinger and J. Weitkamp Wiley-VCH, 1999.
193. M.P. Kiskinova, *Stud. Surf. Sci. Catal.*, 1992, **70**.
194. The term SMSI was introduced by Tauster *et al.* (S.J. Tauster, S.C. Funk, R.L. Garten, *J. Am. Chem. Soc.* 1978, **100**, 170) to denote the effect responsible for the drastic decrease in CO and H<sub>2</sub> chemisorption on titania-supported metals after increasing the reduction temperature from 200 to 500°C. More details on this effect can be found in a review paper of Hadjiivanov and Klissurski (K.I. Hadjiivanov, D.G. Klissurski, *Chem. Soc. Rev.*, 1996, **25**, 61).
195. H. Kolbel and K.D. Tillmetz, *Germ. Pat. Appl.*, 1976, **2**, 507–647.
196. B. Bussemeier, C.D. Frohning and B. Cornils, *Hydrocarbon Process.*, 1976, **56**, 105.
197. B. Bussemeier, C.D. Frohning, G. Horn and W. Kluy, *Germ. Pat. Appl.*, 1976, **2**, 518–964.
198. W.M. van Dijk, J.W. Niemantsverdriet, A.M. Van der Kraan and H.S. Van der Baan, *Appl. Catal.*, 1982, **2**, 273.
199. J. Barrault and C. Renard, *Appl. Catal.*, 1985, **14**, 133.
200. J. Barrault, C. Forquy and V. Perrichon, *Appl. Catal.*, 1983, **5**, 119.
201. R. Malessa and M. Baerns, *Ind. Eng. Chem. Res.*, 1988, **27**, 279.
202. G.C. Maiti, R. Malessa and M. Baerns, *Appl. Catal.*, 1983, **5**, 151.
203. G.Z. Bian, A. Oonuki, N. Koizumi, H. Nomoto and M. Yamada, *J. Mol. Catal. A: Chemical*, 2002, **186**, 203.
204. K.B. Jensen and F.E. Massoth, *J. Catal.*, 1985, **92**, 109.
205. C.K. Das, N.S. Das, D.P. Choudhury, G. Ravichandran and D.K. Chakrabarty, *Appl. Catal. A: General*, 1994, **111**, 119.
206. J. Yang, Y. Lieu, J. Chang, Y.N. Wang, L. Bai, Y.Y. Xu, H.W. Xiang, Y.W. Li and B. Zhong, *Ind. Eng. Chem. Res.*, 2003, **42**, 5066.
207. Y. Liu, J. Yang, L. Bai, Y. Li, L.J. Liu, H.W. Xiang, Y.W. Li and B. Zhong, *Chin. J. Catal.*, 2003, **24**, 299.
208. S.M. Rodulfo-Baechler, S.L. Cortes-Gonzalez, J. Orozco, A.J. Mora and G. Delgado, *Revista Mex. Fisica*, 2003, **49**, 195.
209. M.R. Goldwasser, V.E. Dorantes, M.J. Perez-Zurita, P.R. Sojo, M.L. Cubeiro, E. Pietri, F. Gonzalez-Jimenez, Y.N. Lee and D. Moronta, *J. Mol. Catal. A: Chemical*, 2003, **193**, 227.
210. G.R. Hearne and H. Pollak, *Hyperfine Interact.*, 1991, **67**, 559.
211. N. Koizumi, K. Murai, T. Ozaki and M. Yamada, *Catal. Today*, 2004, **89**, 465.
212. L.Y. Xu, Q.X. Wang, D.B. Liang, X. Wang, L.W. Lin, W. Cui and Y.D. Xu, *Appl. Catal. A: General*, 1998, **173**, 19.
213. J. Abbot, N.J. Clark and B.H. Baker, *Appl. Catal.*, 1986, **26**, 141.
214. E.L. Kugler, S.J. Tauster, S.C.Fung, *US. Pat.* 4,206,134 (1980).
215. S.T. Hussain, *J. Chem. Soc. Pakistan*, 1993, **15**, 97.
216. S.T. Hussain, *J. Chem. Soc. Pakistan*, 1993, **15**, 110.
217. S.T. Hussain, *J. Chem. Soc. Pakistan*, 1993, **15**, 162.
218. S.T. Hussain, *J. Chem. Soc. Pakistan*, 1993, **15**, 234.

219. S.T. Hussain, *J. Chem. Soc. Pakistan*, 1994, **16**, 87.
220. S.T. Hussain, *J. Chem. Soc. Pakistan*, 1995, **17**, 133.
221. S.T. Hussain, *J. Trace Microprobe Techn.*, 1996, **14**, 353.
222. S.T. Hussain, *J. Trace Microprobe Techn.*, 1996, **14**, 361.
223. S.T. Hussain, *J. Trace Microprobe Techn.*, 1996, **14**, 367.
224. S.T. Hussain, *J. Trace Microprobe Techn.*, 1996, **14**, 681.
225. S.T. Hussain, *Ads. Sci. Techn.*, 1996, **13**, 489.
226. S.T. Hussain and M.A. Atta, *Turkish J. Chem.*, 1997, **21**, 77.
227. S.T. Hussain and F. Larachi, *J. Trace Microprobe Techn.*, 2002, **20**, 197.
228. T. Tercioglu and J.F. Akyurtlu, *Appl. Catal. A: General*, 1996, **136**, 105.
229. L.B. Shapovalova and G.D. Zakumbaeva, *Petroleum Chem.*, 2000, **40**, 151.
230. M. van der Riet, G.J. Hutchings and R.G. Copperthwaite, *J. Chem. Soc., Chem. Commun.*, 1986, 798.
231. G.J. Hutchings, M. van der Riet and R. Hunter, *J. Chem. Soc., Faraday Trans. 1*, 1989, **85**, 2875.
232. S.E. Colley, R.G. Copperthwaite, G.J. Hutchings, S.P. Terblanche and M.M. Thackeray, *Nature*, 1989, **339**, 129.
233. Q. Liang, K. Chen, W. Hou and Q. Yan, *Appl. Catal. A: General*, 1998, **166**, 191.
234. M.J. Keyser, R.C. Everson and R.L. Espinoza, *Appl. Catal. A: General*, 1998, **171**, 99.
235. M.J. Keyser, R.C. Everson and R.L. Espinoza, *Ind. Eng. Chem. Res.*, 2000, **39**, 48.
236. S.M. Rudolfo-Baechler, S.L. Gonzalez-Cortes, J. Orozco, V. Sagredo, B. Fontal, A.J. Morea and G. Delgado, *Mater. Lett.*, 2004, **58**, 2447.
237. M. Jiang, N. Koizumi, T. Ozaki and M. Yamada, *Appl. Catal. A: General*, 2001, **209**, 59.
238. T. Riedel, M. Claeys, H. Schulz, G. Schaub, S.S. Nam, K.W. Jun, M.J. Choi, G. Kishan and K.W. Lee, *Appl. Catal. A: General*, 1999, **186**, 201.
239. K. Guse and H. Papp, *Fres. J. Anal. Chem.*, 1993, **346**, 84.
240. D.G. Wickham and W.J. Croft, *J. Phys. Chem. Solids*, 1958, **7**, 351.
241. J.L. Gautier, E. Rios, M. Gracia, J.F. Marco and J.R. Gancedo, *Thin Solid. Films*, 1997, **311**, 51.
242. J.M. Jimenez Mateos, J. Morales and J.L. Tirado, *J. Solid. State Chem.*, 1989, **82**, 87.
243. E. Rios, P. Chartier and J.L. Gaultier, *Solid St. Sci.*, 1999, **1**, 267.
244. E. Vila, R.M. Rojas and O. Garcia-Martinez, *Chem. Mater.*, 1995, **7**, 1716.
245. E. Vila, R.M. Rojas, J.L. Martin de Vidales and O. Garcia-Martinez, *Chem. Mater.*, 1996, **8**, 1078.
246. S. Naka, M. Inagaki and T. Tanaka, *J. Mater. Sci.*, 1972, **7**, 441.
247. F. Morales, O.L.J. Gijzeman, F.M.F. de Groot and B.M. Weckhuysen, *Stud. Surf. Sci. Catal.*, 2004, **147**, 271.
248. F. Morales, F.M.F. de Groot, P. Glatzel, E. Kleimenov, H. Bluhm, M. Havecker, A. Knop-Gericke and B.M. Weckhuysen, *J. Phys. Chem. B*, 2004, **108**, 16201.
249. F. Morales, D. Grandjean, F.M.F. de Groot, O. Stephan and B.M. Weckhuysen, *Phys. Chem. Chem. Phys.*, 2005, **7**, 568.
250. F. Morales, F.M.F. de Groot, O.L.J. Gijzeman, A. Mens, O. Stephan and B.M. Weckhuysen, *J. Catal.*, 2005, **230**, 310.
251. N.N. Madikizela-Mnqanqeni and N.J. Coville, *J. Mol. Catal. A: Chemical*, 2005, **225**, 137.
252. Y. Zhang, M. Koike and N. Tsubaki, *Catal. Lett.*, 2005, **99**, 193.
253. S. Storsaeter, O. Borg, E.A. Blekkan, B. Totdal and A. Holmen, *Catal. Today*, 2005, **100**, 343.

254. S.A. Hosseini, A. Taeb and F. Feyzi, *Catal. Comm.*, 2005, **6**, 233.
255. F.M.T. Mendes, C.A.C. Perez, F.B. Noronha and M. Schmal, *Catal. Today*, 2005, **101**, 45.
256. Y.H. Zhang, H.F. Xiong, K.Y. Liew and J.L. Li, *J. Mol. Catal. A: Chemical*, 2005, **237**, 172.
257. H.F. Xiong, Y.H. Zhang, K. Liew and J.L. Li, *J. Mol. Catal. A: Chemical*, 2005, **231**, 145.
258. T.K. Das, G. Jacobs and B.H. Davis, *Catal. Lett.*, 2005, **101**, 187.
259. A. Infantes-Molina, J. Merida-Robles, E. Rodriguez-Castellon, B. Pawelec, J.L.G. Fierro and A. Jimenez-Lopez, *Appl. Catal. A: General*, 2005, **286**, 239.
260. D.Y. Xu, W.Z. Li, H.M. Duan, Q.J. Ge and H.Y. Xu, *Catal. Lett.*, 2005, **102**, 229.
261. Z.W. Liu, X.H. Li, K. Asami and K. Fujimoto, *Catal. Today*, 2005, **104**, 41.